Three-Body Problem in Nuclear Matter

R. RAJARAMAN*†

Department of Physics, University of Southern California, Los Angeles, California

H. A. BETHE‡

Laboratory of Nuclear Studies, Cornell University, Ithaca, New York

This work reviews some recent developments in the theory of nuclear matter. Assuming familiarity with the basic Brueckner–Goldstone theory described in the preceding article by B. Day, it is first shown that the Brueckner–Goldstone series does not converge in powers of the reaction matrix, and that the perturbation series for the binding energy has to be rearranged in powers of the density ρ. Physical reasons and actual estimates are provided for expecting convergence in powers of ρ.

A detailed theory is outlined for the evaluation of the three-body energy, which gives the ρ^2 term. Attention is paid to both the momentum dependence of the reaction matrix and the tensor nature of nuclear forces. Finally, the last section is devoted to the choice of the single-particle potential energies, suitably designed so as to absorb most of the four-body and higher cluster terms.

CONTENTS

1. INTRODUCTION

Nuclear matter is a uniform system of infinite identical nucleons, stripped of their Coulomb interactions. A study of the properties of this system and in particular the evaluation of its binding energy as a function of its density is a valuable first step towards a theory of realistic finite nuclei starting from first principles. For instance, the binding energy per particle of nuclear matter should give the "volume term" in the well-known semi-emperical mass formula for nuclei, which is experimentally deduced to be about 16 MeV. Further, the experience gained from the treatment of the energy and density of this many-body system should be of great help in evaluating the surface, Coulomb, and other terms in the mass formula.

There are several mathematical formalisms developed for studying nuclear matter. A comparison of these and their relative merits is discussed by Brandow.[1] The most successful, and in many ways the simplest, theory is based on the Brueckner–Goldstone[2,3] formalism. The Hamiltonian is split into

$$H_0=\sum_i(T_i+U_i)$$

and

$$H_1=\sum_{i\neq j} v_{ij}-\sum_i U_i,$$

where T_i are the kinetic energies of the nucleons, v_{ij} are the internucleon potentials, and U_i are single-particle potentials to be chosen conveniently. It is assumed that there are no intrinsic many-body forces. The ground state of H_0 is just that of a zero temperature Fermi gas (it is nondegenerate) and the perturbed wave function and energy are expanded in a perturbation series in powers of H_1. The potentials v_{ij} are used in the form of their reaction matrices, and the resulting series is represented by a set of diagrams similar to the Feynman diagrams. This formalism and the concept of the reaction matrix are explained in the preceding article by Ben Day.

Subsequent to the development of this well-defined formalism, considerable effort has gone into evaluating the lower-order terms and treating higher-order terms in a consistent way. It appears now that the theory is approaching a satisfactory conclusion, both theoretically and in terms of agreement with experiment. One of the significant steps in this process was the development of the Reference Spectrum Method by Bethe, Brandow, and Petschek[4] which provided a relatively simple and analytic method for evaluating the reaction matrix. This also revealed several qualitative features with which higher order diagrams could be studied. Such a study resulted in another significant step, namely the realization that the Brueckner–Goldstone series does not converge in powers of the interaction or the reaction matrix, and that it should be rearranged in powers of the number of nucleons involved.[5,6] The evaluation by Bethe of the three-body energy to all orders in perturbation lends support to the idea that the above re-arrangement in powers of the density should converge for nuclear matter.

Complete calculations using realistic potentials with tensor forces etc. have not yet been fully done. But the work done so far reveals that the sum of the two- and

* Supported in part by the U. S. Atomic Energy Commission under Contract No. AT(04-3)-136; USC Report No. 136-115.

† Present address: The Institute for Advanced Study, Princeton, N.J.

‡ Supported in part by the U. S. Office of Naval Research.

[1] B. H. Brandow, Phys. Rev. **152**, 863 (1966).

[2] K. A. Brueckner and C. A. Levinson, Phys. Rev. **97**, 1344 (1955); K. A. Brueckner, *ibid.* **97**, 1353 (1955).

[3] J. Goldstone, Proc. Roy. Soc. (London) **A293**, 267 (1957).

[4] H. A. Bethe, B. H. Brandow, and A. G. Petschek, Phys. Rev. **129**, 225 (1963), henceforth referred to as BBP.

[5] R. Rajaraman, Phys. Rev. **131**, 1244 (1963).

[6] H. A. Bethe, Phys. Rev. **138**, B804 (1965).

three-body contributions gives a binding energy of about 13 to 18 MeV per particle at the observed density of $k_F = 1.36$ F^{-1} or $\rho = 0.178$ F^{-3}, with the higher binding corresponding to "soft-core" potentials.[7,8] There are reasons to hope that the corrections to this, such as four-body terms, etc., should not be more than a couple of MeV, and methods have been suggested for absorbing these. The experimental value for the binding energy per particle is about 16 MeV. This is a fairly good agreement for a theory beginning from first principles, namely an evaluation of the energy of the many-body system starting from the interparticle potential. In estimating the agreement with experiment one must remember that the theory really calculates the potential energy, which is about -40 MeV for a typical nucleon in the Fermi sea, and that the binding energy is a difference between the large potential and kinetic energies. It is hoped that the uncertainty (and possible discrepancy) of about 3 MeV in a total of about 40 MeV will be reduced by the correction terms and by more precise calculations with tensor forces, etc.

Since the Brueckner–Goldstone formalism and the Reference Spectrum Method for evaluating the reaction matrix have been described in detail in the preceding article by Day,[9] we will proceed from where Day has left off. Thus Sec. 2 will briefly gather together some features of the two-body wave function and the reaction matrix needed for subsequent use. Section 3 will discuss the convergence problems of the expansion and bring out the need to rearrange terms in powers of the density. Sections 4 and 5 will deal with a method for evaluating the three-body energy which gives the ρ^2 term in the new rearrangement. Section 6 involves the treatment of tensor forces, and finally Sec. 7 will be devoted to the choice of the single-particle potential energies to be used in the theory. It is strongly recommended to the reader to familiarize himself with the ideas in the preceding article before embarking on this one.

2. SOME PROPERTIES OF THE TWO-BODY PROBLEM

The Reference Spectrum Method for evaluating the g matrix, described in detail in the preceding article (henceforth referred to as A) can be summarized very briefly as follows:

The g matrix is defined in terms of the internucleon potential v by

$$g = v - v(Q/e)g, \tag{2.1}$$

where Q and e refer, respectively, to the Pauli exclusion operator and the energy denominator in the Goldstone diagram. This is essentially a two-body operator, and involves nontrivially the relative coordinate $\mathbf{r}$, the momenta of the two particles and a parameter which depends on the other particles excited. Let us define a two-body wave function $\psi(\mathbf{r})$ and a defect function $\zeta(\mathbf{r})$ corresponding to an initial plane wave state $\phi(\mathbf{r})$ by

$$\psi(\mathbf{r}) = [1-(Q/e)g]\phi(\mathbf{r}) \tag{2.2}$$

and

$$\begin{aligned}\zeta(\mathbf{r}) &= \phi(\mathbf{r}) - \psi(\mathbf{r}), \\ &= (Q/e)g\phi(\mathbf{r}) = (Q/e)v\psi(\mathbf{r}).\end{aligned} \tag{2.3}$$

The Reference Spectrum approximation,[4] which uses a quadratic form for the single-particle potential energies, amounts to dropping the Q operator, and replacing the energy denominator by $(m^*)^{-1}(-\nabla^2+\gamma^2)$ in coordinate space. These approximations and corrections to them are explained in the original paper[4] and in A. Here m^* refers to the reduced mass in the Reference Spectrum energy, γ^2, a positive quantity, is the parameter involving off-energy-shell contributions from other excited particles, and the factor $\hbar^2/M$ is suppressed. It then follows from (2.3) that

$$(\nabla^2-\gamma^2)\zeta(\mathbf{r}) = -m^*v(\mathbf{r})[\phi(\mathbf{r})-\zeta(\mathbf{r})] \tag{2.4}$$

and the matrix element

$$\begin{aligned}\langle\phi' \mid g \mid \phi\rangle &= \langle \mathbf{k} \mid g \mid \mathbf{k}_0\rangle, \\ &= \langle \mathbf{k} \mid \zeta\rangle[(k^2+\gamma^2)/m^*)].\end{aligned} \tag{2.5}$$

The g matrix element can thus be obtained by solving the differential equation (2.4) as exactly as possible and using the solution for $\zeta(\mathbf{r})$ in (2.5). This has been done quite accurately[4,10] and the first order energy, which is the g matrix itself, has been evaluated. However, for the purposes of studying higher-order diagrams, involving large numbers of g matrices, it is useful to extract some qualitative features of the function ζ and the operator g. The great advantage of the Reference Spectrum Method, as compared to directly solving the integral equation (2.1) for g, is the ease with which it lends itself to such qualitative understanding.

In this connection, it is useful to separate the potential into a short-range part v_s and a long-range part v_l, as originally suggested by Moszkowski and Scott.[11] The separation distance d was so chosen by these workers that the defect function ζ had zero slope and value at $r=d$, i.e., the "wound" in the wave function ψ due to the repulsive core got "healed" at $r=d$ due to the attractive part in v_s. This separation distance is, of course, a function of the initial momenta $\mathbf{k}_0$, $\mathbf{P}_0$.

[7] Such potentials have been suggested by C. W. Wong, Nucl. Phys. **56**, 224 (1964); C. Bressel *et al.*, Bull. Am. Phys. Soc. **10**, 584 (1965); R. V. Reid (private communication).

[8] Calculations using such soft cores have been done by D. Sprung and P. C. Bhargava, Nucl. Phys. (to be published).

[9] B. Day, Rev. Mod. Phys. **39**, 719 (1967), preceding article.

[10] (a) M. Razavy, Phys. Rev. **130**, 1091 (1963); (b) K. A. Brueckner and K. S. Masterson, *ibid.* **128**, 2267 (1962).

[11] S. A. Moszkowski and B. L. Scott, Ann. Phys. (N.Y.) **11**, 65 (1960).

But, for a standard hard core potential, with a core radius $c=0.4$ F, the distance d is about 1 F for a wide range of k_0, P_0 up to about 2 F^{-1}.[12] Moszkowski and Scott show that the reaction matrix g_s corresponding to this v_s is zero for *free* nucleons. Although this is not so for a general off-energy-shell g_s matrix in nuclear matter, it is still useful to make such a separation, since the two parts v_s and v_l have quite different properties and have to be treated differently. v_s contains the strong repulsive core and is best treated in terms of its reaction matrix g_s to get finite matrix elements. Further, because of its short range, g_s has high Fourier components, and, as we will see, a strong momentum dependence. On the other hand, v_l is the relatively weak tail of the attractive part and consequently has a rapidly convergent Born series. Further, although its matrix elements depend strongly on the momentum *transfer*, the diagonal element is relatively independent of momentum. All these properties will be discussed and used in detail at various places in later sections. It should be noted, however, that although such a separation is often useful, it *is* possible to evaluate the g matrix for the full $v(r)$, by solving the differential equation (2.4) for $\zeta(\mathbf{r})$, and this is usually more convenient for accurate numerical work.

The function $\zeta_s(r)$ corresponding to v_s has some useful features. Consider for instance its s-wave part, written as usual in the form $\chi_s^0(r)/r$. Then from (2.4), $\chi_s^0(r)$ obeys

$$[(d^2/dr^2)-\gamma^2]\chi_s^0(r)=m^*v_s(r)[\chi_s^0(r)-rj_0(k_0r)]. \quad (2.6)$$

Inside the hard core, $\psi(r)=0$ and hence $\chi_s^0(r)=rj_0(k_0r)$, the free S-wave function. Outside the core, χ_s^0 falls off to zero slope and value at $r=d$, by definition of d. If there had been no attraction outside the core, then $\chi_s^0(r)=e^{-\gamma r}$ for $r>c$. The attractive part makes the decay of $\chi_s^0(r)$ only faster. Thus, a graph of $\chi_s^0(r)$ has an approximate shape shown in Fig. 1. Inside the core radius, the function $\chi_s^0=rj_0(k_0r)\simeq r$ for small k_0. Deviation from this arises only for large enough k_0 so that $k_0c\sim 1$. Further, outside the core, χ_s^0 does not vary much with k_0, especially for large γ. The largest k_0 dependence outside the core arises from the core boundary value $\chi_s^0(c)=cj_0(k_0c)$. Therefore the outer function, when suitably normalized at the core radius, i.e., either $\chi_s^0(r)/cj_0(k_0r)$ or $\chi_s^0(r)/cj_0(k_0c)$, should be relatively independent of k_0.

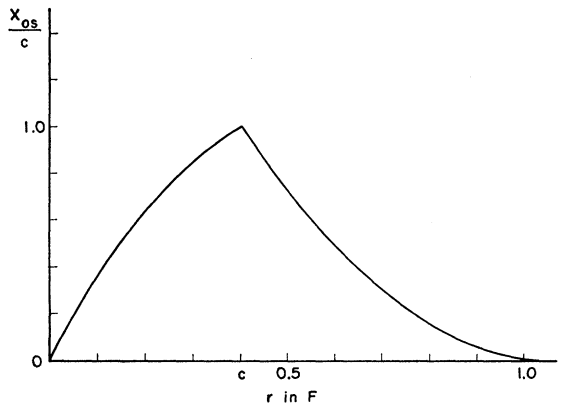

FIG. 1. S-wave part of the two-body defect function for low relative momentum.

[12] The dependence of d on k_0 and P_0, along with several other features of the two- and three-body problems is discussed by M. Kirson, Ph.D. thesis, Cornell University, 1966.

Further, since χ_s^0 is roughly triangular with a peak at $r=c$, its Fourier transform should be peaked around $kc=\pi/2$ i.e., $k\sim 4$ F^{-1}. Thus, when the g_s matrix acts on the filled Fermi sea, it tends to excite intermediate states of momenta typically around 4 F^{-1}. All these features of the defect function will be useful in subsequent discussion.

We can also make similar estimates for the reaction matrix g_s. We have

$$\langle \mathbf{k} \mid g_s/e \mid \mathbf{k}_0\rangle=\langle \mathbf{k} \mid \zeta_s\rangle,$$

$$=\Omega^{-1}\int \exp(-i\mathbf{k}\cdot\mathbf{r})\zeta_s(\mathbf{r})\,d^3r, \quad (2.7)$$

where Ω is the volume of integration. Consider the diagonal case $|\mathbf{k}\rangle=|\mathbf{k}_0\rangle$. The integral in (2.7) can be split into two parts, inside and outside the core radius, respectively. Inside the core, $\zeta_s(\mathbf{r})=\phi(\mathbf{r})=\exp(i\mathbf{k}_0\cdot\mathbf{r})$, so that

$$\int_{\text{core}} \exp(-i\mathbf{k}_0\cdot\mathbf{r})\zeta_s(\mathbf{r})\,d^3r=\int_{\text{core}} d^3r=V_c,$$

the core volume. (2.8)

Outside the core, the contribution is not so trivial, but the shape of χ_s^0 in Fig. 1 shows that the result should be of the same order as the core contribution. An estimate of about $2V_c$ to $3V_c$ is reasonable. Thus,

$$\langle \mathbf{k}_0 \mid (g_s/e) \mid \mathbf{k}_0\rangle=\Omega^{-1}3V_c. \quad (2.9)$$

As an application, consider the first-order direct diagram in g_s. Its contribution, using an average value k_0, is approximately

$$E_s^{(1)}=\tfrac{1}{2}\sum_{m,n<k_F}\langle \mathbf{k}_0 \mid g_s \mid \mathbf{k}_0\rangle$$

$$\simeq\frac{N^2}{2}\left\langle \mathbf{k}_0\left|\frac{g_s}{e}\right|\mathbf{k}_0\right\rangle\frac{(k_0^2+\gamma^2)}{m^*},$$

where N is the number of particles

$$\simeq\tfrac{1}{2}\rho\cdot 3V_c\cdot(k_0^2+\gamma^2)/m^* \text{ per particle.} \quad (2.10)$$

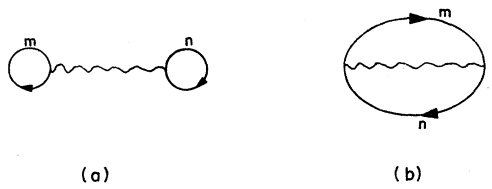

FIG. 2. First-order diagrams.

For purposes of estimation, we can use

$$\rho=0.170\ \mathrm{F}^{-3}\simeq\tfrac{1}{6}\ \mathrm{F}^{-3}, \qquad \text{for } k_F=1.36\ \mathrm{F}^{-1},$$

$$V_c=0.27\ \mathrm{F}^3, \qquad \text{for } c=0.4,$$

$$m^*=1,$$

and $k_0^2+\gamma^2=1.5\ k_F^2$ (see preceding article). This gives the first-order g_s contribution from the "direct" diagram,

$$E_s^{(1)}=\tfrac{1}{2}(0.170)\,(0.81)\,(1.5k_F^2)\simeq 0.10k_F^2\simeq 8\ \mathrm{MeV}$$

per particle.

This is, of course, only an estimate, and is given only to illustrate the essential simplicity of the BBP method. The exact results can always be obtained by solving (2.4) and evaluating (2.5). The estimate in Eq. (2.9) for $\langle \mathbf{k}_0 \mid g_s/e \mid \mathbf{k}_0\rangle$ is very valuable in studying higher order diagrams, as we will see in the next section.

It should be noted here that the first-order contribution of g_s is positive. However, the long-range part v_l makes a large negative contribution (about -59 MeV)[13] through its first Born approximation, so that the full g matrix $g\simeq g_s+v_l$ is negative for small k_0. This gives, then, a positive contribution to the binding energy from the first-order direct diagram.

We further note that since ζ_s is largely k_0-independent, the diagonal g_s matrix element

$$\langle \mathbf{k}_0 \mid g_s \mid \mathbf{k}_0\rangle\simeq[(k_0^2+\gamma^2)/m^*]\langle \mathbf{k}_0 \mid \zeta\rangle$$

has a strong quadratic dependence on k_0. We will see in Sec. 5 that this proves to be a troublesome feature in evaluating the three-body energy, and a full section will be devoted to incorporate this momentum dependence of g_s.

We have described above some selected properties of the two-body wave function and reaction matrix which are needed for the study of higher orders that follows. The reader is referred to the preceding article for fuller details of the two-body problem.

3. THE CONVERGENCE OF THE BRUECKNER-GOLDSTONE SERIES

We will study in this section the convergence of the Brueckner–Goldstone expansion order by order. In general, the expansion will contain diagrams involving the single-particle potential energy U (see A). Obviously, their contribution will depend on the choice of U, which in turn depends on what pure g matrix diagrams one is trying to cancel out by these "U diagrams." Therefore let us first concentrate on diagrams that do not involve U.

The first-order diagrams are shown in Fig. 2. Here, Fig. 2(b) is the "exchange" of 2(a). In the previous section, we made a crude estimate of the direct diagram 2(a) as

$$\tfrac{1}{2}\rho\sum_{\mathbf{mn}}(g_s+v_l)\simeq+8-59\ \mathrm{MeV}=-51\ \mathrm{MeV}.$$

The exchange diagram can be similarly evaluated. However, one can see that the exchange diagram is "almost" diagonal, inasmuch as the momentum transfer $\mathbf{m}-\mathbf{n}$ is quite small, so that for a given $\mathbf{m}$ and $\mathbf{n}$, it should not be very different from the direct term. But, for a spin–isospin-independent potential, the states $\mathbf{m}$ and $\mathbf{n}$ must have the same spin–isospin values in the exchange diagram. Consequently, the exchange diagram contribution is multiplied by an additional factor of $-\frac{1}{4}$, the minus sign arising from the Goldstone rule mentioned in A. As a result, the total first-order contribution should be about $\frac{3}{4}$ the direct term, i.e., about -39 MeV. We wish to emphasize again, that whereas the ease with which such estimates can be made is the great advantage of the BBP method, it is always possible to get more exact answers by solving the differential equation for $\zeta(\mathbf{r})$. A recent such calculation by Kirson[12] gives a value of -38.35 MeV for the first-order energy, using the standard hard-core potential, in very close agreement with our estimate.

There are no second-order diagrams in the Brueckner–Goldstone expansion. The third-order direct diagrams are only a handful, as shown in Fig. 3. The remaining

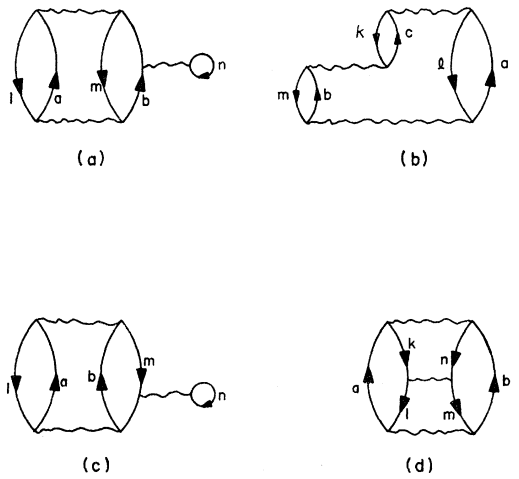

FIG. 3. Third-order direct diagrams.

[13] R. Rajaraman, Phys. Rev. 155, 1105 (1967).

third-order diagrams can be obtained by simply "exchanging" one or more of the g matrices in Fig. 3. Of the third-order diagrams, Fig. 3(a) and Fig. 3(c) caught early attention, inasmuch as they seemed to represent self-energy effects. The "bubble interaction" $\langle bn \mid g \mid bn \rangle$ in Fig. 3(a), for example, when summed over the state n, may be considered as part of the single-particle energy of the state b, and might therefore be counteracted by a suitable $U(b)$. A similar statement would be valid for Fig. 3(c), where the "bubble interaction" $\langle mn \mid g \mid mn \rangle$ may be included as part of the hole energy $U(m)$. This method, which corresponds to the Hartree method in atomic physics, is explained in Goldstone's paper,[3] and forms the basis of the BBP choice of their single-particle energies. The BBP choice, which will be discussed in Sec. 7, absorbs, on the average, diagrams 3(a), 3(c) and their exchanges, as part of the single-particle energies.

Concurrently, it was shown by Rajaraman[14] that the remaining third-order diagrams are comparable in size to the bubble diagrams, and should be taken into account to make a consistent approximation. However, he also showed that even though these are not obviously self-energy type diagrams, more than 90% of their contribution could still be absorbed into the single-particle energies. These additional diagrams were then included by BBP in determining their reference spectrum parameters. The spirit of the efforts at that time was still based on the hope that the Brueckner–Goldstone series converges as you go to higher order diagrams in g, and that if you have accounted for all third-order diagrams in the above manner, this should leave only small errors from fourth- and higher-order terms.

However, when calculations were performed by Razavy[10a] for the first-order energy with such a single-particle spectrum, the resulting binding energy was only about 8 MeV per particle. Razavy used the Hamada–Johnston potential.[15] A similar result was obtained by Brueckner and Masterson[10b] using the (very similar) Breit potential. However, Brown, Schappert, and Wong[16] showed that both the Razavy result and the Brueckner–Masterson (Br–M) result needed corrections, which coincidentally reduced both values down to about 4 MeV or so. In particular, the Br–M calculations did not include the off-energy-shell effects on the single-particle energies. More recently Coon and Dabrowski[17] have incorporated the off-energy-shell corrections into the Br–M energies. It should be noted in this connection that use of *both* the Coon–Dabrowski and the Brown *et al.* corrections to the Br–M calculations is wrong since these corrections duplicate one another. It should also be remembered that Coon–Dabrowski inclusion of off-energy-shell effects into the single-particle energies had already been achieved earlier by the BBP spectrum.

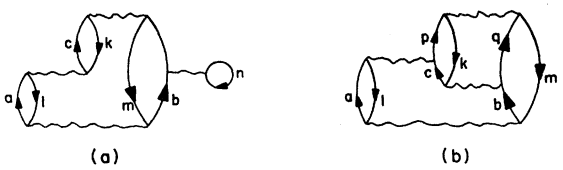

FIG. 4. Two fourth-order diagrams. Diagram (a) contains one extra independent hole line as compared to Fig. 3(b), while diagram (b) has an extra particle line.

A number of further calculations have been carried out by the Japanese school, taking properly into account the off-energy-shell effects using the BBP method. In these calculations, many different potentials are compared, including Hamada–Johnston, an old Gammel–Thaler potential, and some new potentials[18] with small or soft repulsive cores. The softer potentials gave generally greater binding energy, as expected, but none gave the full 16 MeV.

These remarks are a digression from our main point that the sum of the first- and third-order energies after these corrections give only about 4 MeV of binding per particle as compared to the experimental value of 16 MeV.

This can be improved upon by using a "soft-core" repulsion, such as the exponential core of Wong,[7] instead of the infinite "hard core." This would clearly decrease the repulsion, and was estimated by Wong to add about 4–5 MeV to the binding energy. This still leaves a discrepancy of over 7 MeV, the cause of which turned out to be connected with the underlying hope that the Brueckner–Goldstone series converged order by order.

This hope turned out to be quite false, as a closer inspection of higher order diagrams revealed. It was shown by Rajaraman[5] that there exist, in the expansion, subsets of diagrams characterized by the number of hole lines in them, where higher and higher order terms in each subset do not become smaller, so that evaluating the series order by order is not the proper procedure. It was also suggested that each of these subsets should be summed in coordinate space and that the resulting sequence, corresponding to an increasing number of hole lines, will converge. We will now outline these arguments.

Consider the two fourth order diagrams in Fig. 4. Compare both of these to the third-order diagram in Fig. 3(b). Figure 4(a) has one more factor g/e (the

[14] R. Rajaraman, Phys. Rev. **129**, 265 (1963).
[15] T. Hamada and I. D. Johnston, Nucl. Phys. **34**, 383 (1962).
[16] G. E. Brown, G. T. Schappert, and C. W. Wong, Nucl. Phys. **56**, 191 (1964).
[17] S. Coon and J. Dabrowski, Phys. Rev. **140**, B287 (1965).
[18] Y. Akaishi, K. Takada, and S. Takagi, Progr. Theoret. Phys. (Kyoto) **36**, 1135 (1966); Harada, Tamagaki, and Tanaka, *ibid.* **36**, 1003 (1966); K. Takada, S. Takagi, and W. Watari, *ibid.* (to be published). These papers also give references to Japanese work on nuclear potentials with small or soft cores.

"bubble" interaction) and has to be integrated over one more independent state, namely n, as compared to Fig. 3(b). Of course, the contribution of a diagram involves integrals over all the intermediate state momenta, and although the integrand $ge^{-1}ge^{-1}ge^{-1}g$ factors into contributions of the individual g matrices, the integrated result will not. Nevertheless, for purposes of making estimates, we can write

$$\frac{\text{diagram 4(a)}}{\text{diagram 3(b)}}$$

$$\simeq \sum_{n<k_F} \langle \mathbf{bn} \mid g/e \mid \mathbf{bn} \rangle \qquad \text{with a typical } b\sim 4\ \mathrm{F}^{-1},$$

$$\simeq \rho \langle \mathbf{k}_0 \mid g/e \mid \mathbf{k}_0 \rangle \qquad \text{with } \mathbf{k}_0=\tfrac{1}{2}(\mathbf{b}-\mathbf{n}). \quad (3.1)$$

This is where our estimates for $\langle \mathbf{k}_0 \mid g/e \mid \mathbf{k}_0 \rangle$ at the end of the last section are very useful. There we showed that

$$\langle \mathbf{k}_0 \mid g/e \mid \mathbf{k}_0 \rangle = \langle \mathbf{k}_0 \mid \zeta \rangle$$

gives a core contribution of V_c, and something of the same order ($2V_c$ to $3V_c$) from outside the core. Thus,

$$\frac{\text{diagram 4(a)}}{\text{diagram 3(b)}} \simeq 3.5\rho V_c = 3.5(c/r_0)^3 \simeq \tfrac{1}{7}, \quad (3.2)$$

where $2r_0$ = interparticle distance = 2.24 F. Consider, on the other hand, the diagram 4(b). Here again we have an additional factor of g/e as compared to Fig. 3(b), but the additional independent momentum to be integrated over, whether it be p or q, is above the Fermi sea. Thus,

$$\frac{\text{diagram 4(b)}}{\text{diagram 3(b)}} \simeq \sum_{p>k_F} (g/e).$$

As we showed in the last section, the typical particle momentum p excited by the g matrix is about $\pi/2c \simeq 4$ F^{-1}. This we justified by considering the Fourier transform of $\zeta(r)$, and the large value of the momentum was seen to arise because of the hard core. Thus, even though the matrix element g/e is of the same order as before, the phase space over which this is integrated is much larger than the Fermi sea, and we would get a result

$$\frac{\text{diagram 4(b)}}{\text{diagram 3(b)}} \simeq 3.5[c(\pi/2c)]^3. \quad (3.3)$$

On detailed consideration, this factor turns out to be an overestimate inasmuch as g/e is smaller than 3.5 V_c for high momenta, and the typical momentum p is somewhat smaller than $\pi/2c$. However, this ratio is at least of the order of unity, as compared to the ratio of $\frac{1}{7}$th in Eq. (3.2). A better way of estimating this ratio is given by Day.[9] We have

$$\frac{\text{diagram 4(b)}}{\text{diagram 3(b)}} \simeq \sum_k \langle \mathbf{k} \mid Qg/e \mid \mathbf{k}_0 \rangle = \sum_k \langle \phi_k \mid \zeta_0 \rangle, \qquad \text{where } \mid \mathbf{k} \rangle = \mid \phi_k \rangle = \exp(i\mathbf{k}\cdot\mathbf{r}),$$

$$= \sum_k (\phi_k \text{ at } r=0)\langle \phi_k \mid \zeta_0 \rangle, \qquad \text{since } \phi_k(0)=1,$$

$$= \zeta_0(r=0) = \phi_k(r=0) = 1.$$

Once again we see that this ratio arises because $\zeta(r=0)=\phi_k(r=0)$, which in turn is because of the hard core. The argument used here in going from third to fourth order, is clearly valid at all orders. We conclude then, that in going to a diagram of next higher order, if the extra independent intermediate state introduced is a particle, the higher-order diagram remains of the same size, whereas if the intermediate state is a hole, then there is a reduction by about a seventh.

The above convergence behavior becomes more transparent when summarized in direct physical terms thus:

With an infinite hard core in the potential, we must, of course, anticipate convergence problems in powers of the potential. In fact, if we use the potential as it is, even the matrix elements diverge. The situation is improved by the use of the reaction matrix g, which is at least finite. This renders every diagram in powers of g finite. However, this does not imply that such a sequence of finite diagrams will converge order by order. Now, if a diagram contains n hole lines, it corresponds to an interaction between n particles, since it is easy to note that every hole line corresponds to one particle being excited out of the Fermi sea. Since it is the hard core which leads to convergence problems, and since the probability of a large number of particles being within each other's core radius is small ($\rho c^3<1$), we would expect a diagram to get smaller as the number of hole lines increases. But if the number of hole lines is kept constant and the number of g matrices is increased by adding particle lines only, then there is not likely to be good convergence. Our semiquantitative arguments earlier simply corroborate this conjecture. This possibility of convergence in powers of the density had been suggested as early as 1957 by Hugenholtz.[19]

[19] N. M. Hugenholz, Physica **23**, 533 (1957).

At this juncture, it is again helpful to separate the potential into v_s and v_l. An arbitrary diagram would then consist of an arbitrary sequence of v_s and v_l interactions, and if uninterrupted two-body ladders of v_s are summed into g_s as usual, then we have diagrams with arbitrary combinations of g_s and v_l. These may be separated into three classes. (a) Diagrams involving v_l alone. These will be very small inasmuch as the second Born term in v_l is seen to be 2% of the first.[11,12] The reason[13] behind this large dimunition will be clear in Sec. 7. (b) Diagrams mixed in v_l and g_s. We will show in Sec. 7 that these can be absorbed into the single-particle energies. (c) Diagrams involving g_s alone. It is these diagrams which, owing to the hard core, lead to a nonconvergent sequence for a fixed number of hole lines, for the reasons outlined.

Nevertheless, if you consider one such sequence, say, of all diagrams with three hole lines, i.e., the three-body clusters, then the contributions of successive orders alternate in sign. That is, a seventh order diagram as compared to a sixth order one, would contain an extra factor $[Q/(E_0-H_0)]g_s \simeq g_s/-e$ which is negative since g_s is positive. Thus, it is possible that the sequence may have a finite sum.

This was in fact shown to be the case. We will use now a convention for drawing diagrams introduced by Rajaraman for handling n-body cluster diagrams. Every nucleon is represented by a vertical line, with interactions represented by horizontal lines or wiggles as before. "Particle" and "hole" states are distinguished only by arrows. A Goldstone diagram and its representation in the new convention are shown in Fig. 5. The disadvantage of the new convention is that it does not distinguish between particle and hole states very clearly. On the other hand, it brings out the unity of all n-body diagrams of all orders. Thus, all three-body diagrams are "ladders" with these vertical lines. This already suggests that all these three-body ladders may be summed in a manner similar to Brueckner's summation of all two-body v-ladders into a g matrix. It was shown[5] that the sum of such three-body ladders, called the T matrix, is finite and can be evaluated in a manner similar to the reference spectrum method for the two-body g matrix. A three-body wave function analogous to $\psi^{\text{Reference}}$ can be defined, which obeys a three-body Schrödinger type differential equation. If this equation can be solved, then the T matrix, or the three-body energy, can be easily obtained. The same procedure can be adopted for four-body and higher cluster diagrams. Whereas the corresponding n-body Schrödinger-type equations would be harder and harder to solve as n increases, the solution nevertheless exists and leads to finite energies for the contribution of all the n-body diagrams. Furthermore, in view of the short-range nature of g_s, these contributions should converge as n increases.

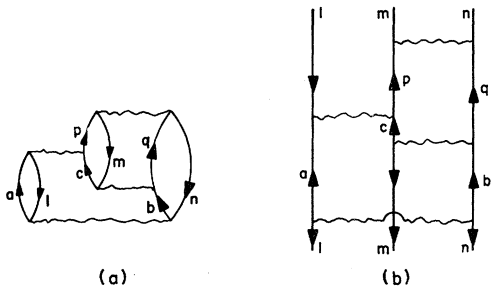

FIG. 5. A fourth-order term represented in (a) the Goldstone convention, and (b) the Rajaraman convention.

Although Rajaraman's work suggested the above possibilities, it did not attempt the actual solution of the three-body differential equation to get the three-body energy. This was done a year later by Bethe,[6] who, with the help of Faddeyev's technique,[20] obtained a satisfactory solution to the three-body wave function and energy. This work also revealed in greater detail the above convergence difficulties, and the effect of going from third order to all three-body terms. We will describe this work in detail in the next section. We only need to mention here that Bethe's work, subsequently further improved by Day[21] and Kirson,[12] leads to a three-body energy of about -5 MeV, which, compared to the -38.3 MeV for the two-body energy, indicates a good rate of convergence in the cluster expansion, thus giving us hope that the four-body energy would be less than 1 MeV.

4. THE THREE-BODY ENERGY

We will now discuss a method for determining the three-body wave function and energy in nuclear matter, developed by Bethe in 1964.[6] The wave function and energy correspond to the sum of all Goldstone diagrams with three hole lines. We will use the convention[5] mentioned in the last section for drawing cluster diagrams, whereby all three-hole-line diagrams will consist of three upgoing lines. The interactions g are wiggly horizontal lines as before, and energy denominators are just the energies of the intermediate states shown minus the starting energies, as can be verified by comparing the two diagrams in Fig. 5. Subject to a handful of exceptions, the set of all allowed three-hole-line Goldstone diagrams is just the set of all possible three-body ladders one can draw, in the new convention. The exceptions arise because there are some "three-hole" Goldstone diagrams, such as the "hole–bubble" diagram in Fig. 3(c), which cannot be represented as part of the ladder sequence, and conversely there are a few ladder diagrams that have no Goldstone ana-

[20] L. D. Faddeyev, Zh. Eksperim. i Teor. Fiz. **39**, 1459 (1960); Dokl. Akad. Nauk SSSR **138**, 565 (1961) [English transls.: Soviet Phys.—JETP **12**, 1014 (1961); Soviet Phys.—Dokl. **6**, 384 (1962), respectively.

[21] B. E. Day, Phys. Rev. **151**, 826 (1966).

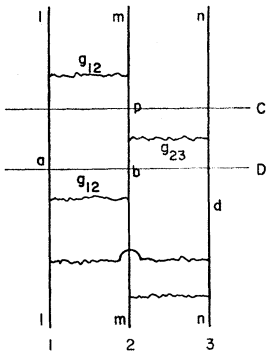

FIG. 6. A typical three-body cluster term belonging to $\langle lmn \mid T \mid lmn \rangle$.

logs and should be subtracted away. These anomalies will be taken into account later on, but let us for the moment consider the sum of all three-body ladder diagrams.

Let us denote by T, the matrix denoting the sum of all three-body ladders, analogous to the g matrix for the two-body ladders. In other words, $\langle \mathbf{lmn} \mid T \mid \mathbf{lmn} \rangle$ is the sum of all three-body diagrams that begin and end on states l, m, and n, respectively. Since binding energy diagrams are "vacuum to vacuum" in the second quantized language, the states **l**, **m**, and **n** are below the sea. We will start by evaluating only direct diagrams, i.e., where the three particles are restored to the same respective state in which they started. Exchange diagrams, belonging for instance to $\langle \mathbf{mln} \mid T \mid \mathbf{lmn} \rangle$ are related in a fairly simple way to the direct diagrams, as in the two-body case, and will be dealt with later. Needless to say, except for the initial and final states **l**, **m**, **n**, all other states in the ladders should be above the Fermi sea, and no two successive g matrices should refer to the same pair of intermediate states. These rules are directly carried over from Goldstone diagrams. Figure 6 shows a typical diagram belonging to $\langle \mathbf{lmn} \mid T \mid \mathbf{lmn} \rangle$. Clearly this set of diagrams can be divided into three distinct groups depending on which pair of particles is involved in the last g interaction. Let us define $T^{(1)}$, $T^{(2)}$, and $T^{(3)}$ to be the sum of the group of diagrams in whose last interaction the particle 1, 2, and 3, respectively, is a spectator. Clearly,

$$T = T^{(1)} + T^{(2)} + T^{(3)}. \tag{4.1}$$

Such a separation was suggested by Faddeyev[20] in connection with the three-body scattering matrix. Now, a diagram belonging to $T^{(3)}$, such as the one in Fig. 6, must have g_{12} as its last interaction. The next lower interaction must therefore be either g_{13} or g_{23}. Thus, the part of the diagram below the g_{12} itself corresponds to a term in either $T^{(1)}$ or $T^{(2)}$. The only exception to this is if there is no interaction at all below g_{12}, i.e., if the entire diagram corresponds only to g_{12}. Thus,

$$T^{(3)} = g_{12} - g_{12} e^{-1} \{ T^{(1)} + T^{(2)} \} \quad \text{and cyclic permutations.} \tag{4.2}$$

The first term on the right-hand side, g_{12}, which corresponds to the third particle not interacting at all, is really part of the two-body energy and is an example of the unwanted exceptions we spoke of earlier. We will eventually subtract away its effect from $T^{(3)}$.

Equation (4.2) and its two cyclic permutations form a set of three, coupled, integral equations for $T^{(1)}$, $T^{(2)}$, and $T^{(3)}$. As in the case of the two-body g matrix, these integral equations are best solved by transforming the problem into coordinate space and solving for suitably defined wave functions. It should be noted that in Eq. (4.2) we have dropped the exclusion operator Q which would ensure that the intermediate states of particles 1 and 2 remain above the sea. This approximation is similar to the one made in A for the two-body g matrix and is justified by the same arguments. The single-particle energies that go into the denominator e are given by the same reference spectrum as in the two-body case.

Let us now define three-body wave functions $\Psi^{(i)}$ by

$$T^{(3)} \Phi = g_{12} \Psi^{(3)}, \quad \text{and cyclic permutations,} \tag{4.3}$$

where Φ is the unperturbed plane wave three-particle state. It follows from Eq. (4.2) that

$$\begin{aligned} \Psi^{(3)} &= [1 - e^{-1} \{ T^{(1)} + T^{(2)} \}] \Phi, \\ &= \Phi - e^{-1} \{ g_{23} \Psi^{(1)} + g_{13} \Psi^{(2)} \}, \quad \text{and cyclic permutations.} \end{aligned} \tag{4.4}$$

The wave functions $\Psi^{(i)}$ and the above equation (4.4) are the three-body analogues of $\Psi(\mathbf{r})$ and its equation (2.2) for the two-body case. As in the two-body case, if we convert $e^{-1} g_{ij}$ into differential operators in the variables $\mathbf{r}_{ij}$, then (4.4) would give a set of coupled differential equations for $\Psi^{(i)}$.

The operator e, deceptive in its abbreviated form, is more complicated than in the two-body case. In every three-body diagram, the first and last energy denominators correspond to two nucleons being excited and the third below the sea. Thus, in Fig. 6, at the level C, nucleons 1 and 2 are in excited states **a** and **p** whereas 3 has returned to the state **n** below the sea. Every energy denominator except the first and the last, such as at level D in Fig. 6, corresponds to all three nucleons in excited states. Using the reference spectrum[22] (see A) both types of energy denominators can be expressed in the form $(m^*)^{-1}(-\nabla_{ij}^2 + \gamma^2)$, but the value of γ, using typical values for all the momenta involved, is higher when all three nucleons are excited. To be more explicit, at level D,

$$\begin{aligned} e &= E(a) + E(b) + E(d) - E(l) - E(m) - E(n), \\ &= (2m^*)^{-1} [a^2 + b^2 + d^2 - l^2 - m^2 - n^2 + 6\Delta k_F^2], \\ &= (m^*)^{-1} [k_{ab}^2 + P_{ab}^2 + \tfrac{1}{2}(d^2 - l^2 - m^2 - n^2) + 3\Delta k_F^2]. \end{aligned}$$

[22] This is the BBP spectrum described in A. Briefly, we will use it in the form $E(b) = (m^*)^{-1}(b^2) + A_2$ for $b > k_F$ and $E(n) = (m^*)^{-1} n^2 + A_1$ for $n < k_F$ with Δ defined by $A_2 - A_1 = \Delta k_F^2$.

But $\mathbf{P}_{ab}=\frac{1}{2}(\mathbf{a}+\mathbf{b})=\frac{1}{2}(\mathbf{l}+\mathbf{m}+\mathbf{n}-\mathbf{d})$ by momentum conservation.

$P_{ab}^2=\frac{1}{4}(l^2+m^2+n^2+d^2)$ averaging over angles,

$$e=(m^*)^{-1}[k_{ab}^2+\tfrac{1}{4}(3d^2)-\tfrac{1}{4}(l^2+m^2+n^2)+3\Delta k_F^2],$$
$$=(m^*)^{-1}[-\nabla_{12}^2+\tfrac{1}{4}(3d^2)+(3\Delta-0.45)k_F^2]. \quad (4.5)$$

Using $\langle l^2\rangle=\langle m^2\rangle=\langle n^2\rangle=0.6k_F^2$, thus

$$e=(m^*)^{-1}(-\nabla_{12}^2+\gamma_1^2),$$

with

$$\gamma_1^2=\tfrac{1}{4}(3d^2)+(3\Delta-0.45)k_F^2. \quad (4.6)$$

The value of the particle momentum d can be typically taken as $\sim\pi/2c$ from the arguments in Sec. 2 for the most probable momenta excited.

On the other hand, at the level C in Fig. 6, where only two particles are excited, the energy denominator is on the energy shell, i.e.,

$$e=E(a)+E(p)-E(l)-E(m),$$
$$=(m^*)^{-1}[k_{ap}^2-k_{lm}^2+2\Delta k_F^2],$$
$$=(m^*)^{-1}(-\nabla_{12}^2+\gamma_2^2), \quad (4.7)$$

where

$$\gamma_2^2=2\Delta k_F^2-k_{lm}^2$$
$$=(2\Delta-0.3)k_F^2\ll\gamma_1^2. \quad (4.8)$$

Therefore, even using average values for the momenta involved, there are two distinct energy denominators, similar in form, but with different γ's. In either case, we know from Sec. 2 how $e^{-1}g_{ij}$ operates on the two-body plane wave state. It effects only the relative coordinate r_{ij} and gives

$$e^{-1}g_{ij}\{\exp[i(\mathbf{k}\cdot\mathbf{r}_{ij}+2\mathbf{P}\cdot\mathbf{R}_{ij})]\}$$
$$=\zeta_{k,P}(\mathbf{r}_{ij})\exp(2i\mathbf{P}\cdot\mathbf{R}_{ij}), \quad (4.9)$$

where $\zeta_{k,P}(\mathbf{r}_{ij})$ can be obtained from (2.4) and its general features such as "healing" etc. were discussed. Clearly ζ depends on the value of γ; let us use the symbol η to denote this function when $\gamma=\gamma_2$ and ζ itself when $\gamma=\gamma_1$. To incorporate the distinction between $\eta(\mathbf{r}_{ij})$ and $\zeta(\mathbf{r}_{ij})$, the former occurring when two particles are excited and the latter when all three are, we split the $\Psi^{(i)}$ in Eq. (4.4) into $(\Psi^{(i)}-\Phi)$ and Φ. When $e^{-1}g_{ij}$ acts on Φ, clearly only the ith and jth particle are excited. Hence

$$e^{-1}g_{ij}\Phi=\eta(\mathbf{r}_{ij}). \quad (4.10)$$

Here we have used the limit of zero momenta for all hole states, so that $\Phi=1$. This approximation, reasonable inasmuch as the average hole momentum is

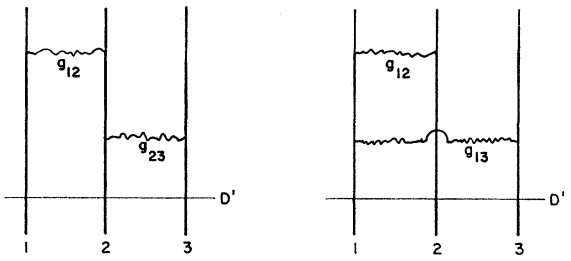

FIG. 7. Two "three-body ladder" diagrams which have no Goldstone analog.

$(0.3)^{1/2}k_f\approx 1/3c$, will be used in all subsequent discussion. Thus, Eq. (4.4) becomes

$$\Phi-\Psi^{(3)}=e^{-1}g_{23}\Phi+e^{-1}g_{13}\Phi-e^{-1}g_{23}(\Phi-\Psi^{(1)})$$
$$-e^{-1}g_{13}(\Phi-\Psi^{(2)})$$

or

$$Z^{(3)}=\eta(\mathbf{r}_{23})+\eta(\mathbf{r}_{13})-e^{-1}g_{23}Z^{(1)}-e^{-1}g_{13}Z^{(2)}, \quad (4.11)$$

where $Z^{(i)}=\Phi-\Psi^{(i)}$. We thus have to solve the three coupled differential equations implied in (4.11), for the $Z^{(i)}$. Since each $Z^{(i)}=\Phi-\Psi^{(i)}$ represents an excited wave function with no initial state in it, the operation of $e^{-1}g_{ij}$ on it will involve only the function $\zeta(\mathbf{r}_{ij})$, and not $\eta(\mathbf{r}_{ij})$.

However, the $Z^{(i)}$ are functions of all three coordinates. Therefore, to find the result of operating $e^{-1}g_{12}$ on $Z^{(3)}(\mathbf{r}_1,\mathbf{r}_2,\mathbf{r}_3)$, one must first Fourier-analyse $Z^{(3)}$, replace $\exp(i\mathbf{k}\cdot\mathbf{r}_{12})$ by $\zeta_{k,P}(\mathbf{r}_{12})$ in each Fourier component, and then perform the inverse Fourier transformation. The resulting function is of course not related in any simple way to $Z^{(3)}(\mathbf{r}_1,\mathbf{r}_2,\mathbf{r}_3)$ and the coupled equations (4.11) are not easy to solve. Consequently, two approximations, a simpler one due to Bethe and an improved version due to Day, have been suggested for obtaining the $Z^{(i)}$. We will present both of them here. Once the $Z^{(i)}$ are known, the three-body energy is easily obtained in terms of these functions. Thus $\langle lmn\mid T^{(3)}\mid lmn\rangle$ is just the sum of all diagrams of the type in Fig. 6, which end with g_{12} and have all possible combinations of g_{ij} underneath with one exception. The diagrams shown in Fig. 7 have no analogs in the Goldstone series since they do not conserve momentum. Noting that the state at the level D in Fig. 6 is $\Psi^{(1)}$, whereas it is Φ at level D in Fig. 7, we get, on removing the term of Fig. 7,

$$\langle lmn\mid T^{(3)}\mid lmn\rangle=\langle\Phi\mid g_{12}(-e)^{-1}\mid g_{23}\Psi^{(1)}+g_{13}\Psi^{(2)}\rangle$$
$$-\langle\Phi\mid g_{12}(-e)^{-1}(g_{23}+g_{13})\mid\Phi\rangle,$$
$$=\langle\Phi\mid g_{12}e^{-1}\mid g_{23}Z^{(1)}+g_{13}Z^{(2)}\rangle,$$
$$=\frac{1}{\Omega^3}\int\eta(\mathbf{r}_{12})\{g(\mathbf{r}_{23})Z^{(1)}(\mathbf{r}_1\mathbf{r}_2\mathbf{r}_3)$$
$$+g(\mathbf{r}_{13})Z^{(2)}(\mathbf{r}_1\mathbf{r}_2\mathbf{r}_3)\}d\tau_1\,d\tau_2\,d\tau_3, \quad (4.12)$$

where Ω is the volume of integration.

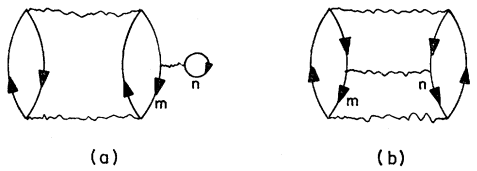

FIG. 8. Two Goldstone diagrams in third order, which are not contained in $\langle lmn \mid T \mid lmn \rangle$.

Some comments are due concerning equation (4.12). In deriving it, we have explicitly written out two powers of g, i.e., the top two "rungs" of the three-body ladder, and left the rest in the wave functions $Z^{(1)}$ and $Z^{(2)}$. To be more precise, we have written

$$\langle lmn \mid T^{(3)} \mid lmn \rangle = \langle \Phi \mid g_{12}e^{-1} \mid g_{23}Z^{(1)}+g_{13}Z^{(2)} \rangle \quad (4.13)$$

instead of the original definition

$$\langle lmn \mid T^{(3)} \mid lmn \rangle = \langle \Phi \mid g_{12} \mid \Psi^{(3)} \rangle. \quad (4.14)$$

There are many reasons for this. First of all, this explicitly brings out the last energy denominator which corresponds to two excited particles, and leads to $\langle \Phi \mid g_{12}e^{-1} = \langle \eta_{12} \mid$. Secondly, the pure two-body term $\langle \Phi \mid g_{12} \mid \Phi \rangle$ present in (4.13) has been removed in (4.14). Thirdly, of course, the unwanted diagrams in Fig. 7 have also been removed by the use of $Z^{(1)}$ and $Z^{(2)}$ instead of $\Psi^{(1)}$ and $\Psi^{(2)}$.

It should also be noted that the g matrix is not a function of the coordinates alone, as assumed in the last line of (4.12). Whereas at large distances $g(\mathbf{r}) \rightarrow v(\mathbf{r})$, at short distances g is highly momentum-dependent. As shown in Sec. 2 and in Day's preceding article, one may write

$$e^{-1}g\Phi = \zeta,$$

where, inside the core, $\zeta = \Phi$. Hence, inside the core $g = e = (m^*)^{-1}(k^2+\gamma^2)$ in the reference approximation, where k is the momentum corresponding to the relative coordinate r in $g(r)$. Incorporating this momentum dependence is complicated by the fact that the integral (4.12) involves $g(\mathbf{r}_{23})$, which depends on k_{23}, along with functions $\eta(\mathbf{r}_{12})$ and $Z^{(1)}(\mathbf{r}_1\mathbf{r}_2\mathbf{r}_3)$, which involve other coordinates. This problem will be discussed in Sec. 5. For the time being let us consider the $g(\mathbf{r}_{23})$ and the $g(\mathbf{r}_{13})$ in (4.12) to be independent of momentum, but evaluated at a suitable average value of the relevant momentum. Finally, as mentioned at the beginning of this section, there are some Goldstone diagrams which are not present in such "ladder" sequences. For the three-body case, the sum $T^{(1)}+T^{(2)}+T^{(3)}$ defined above does not include the "hole–bubble" diagram and the "hole–hole" diagram shown in Fig. 8(a) and 8(b), respectively. However, Fig. 8(a) is a component of the standard expression for the potential energy of hole states (see also Sec. 7). Diagram 8(b) can be explicitly calculated by integrating the product of the three g matrices over the independent momenta. This diagram has been shown by Rajaraman[14] to be smaller by a factor of about $\frac{1}{3^2}$ compared with 8(a); it could probably be absorbed into $U(m)$ and $U(n)$.

Subject to these remarks, $T^{(3)}$ and similarly $T^{(1)}$ and $T^{(2)}$ can be evaluated from Eq. (4.12), once the functions $Z^{(i)}(\mathbf{r}_1\mathbf{r}_2\mathbf{r}_3)$ are known. Let us now proceed to evaluate these functions from the coupled equations (4.11).

Three-Body Wave Function

It is useful to change the coordinates in (4.11) from $\mathbf{r}_1$, $\mathbf{r}_2$, $\mathbf{r}_3$ to $\mathbf{r}_{12} = \mathbf{r}_1 - \mathbf{r}_2$, $\boldsymbol{\varrho}_3 = \frac{1}{2}(\mathbf{r}_1+\mathbf{r}_2) - \mathbf{r}_3$. We then have,

$$e^{-1}g_{12}Z^{(3)}(\mathbf{r}_{12}, \boldsymbol{\varrho}_3, \mathbf{r}_3) = Z_g^{(3)}(\mathbf{r}_{12}, \boldsymbol{\varrho}_3, \mathbf{r}_3),$$

$$= 8(2\pi)^{-6} \int d^3P \int d^3k \zeta_{\mathbf{k},\mathbf{P}}(\mathbf{r}_{12})$$

$$\times \exp(i2\mathbf{P}\cdot\boldsymbol{\varrho}_3) Z_T^{(3)}(\mathbf{P}, \mathbf{k}, \mathbf{r}_3), \quad (4.15)$$

where $Z_T^{(3)}(\mathbf{P}, \mathbf{k}, \mathbf{r}_3)$ is the Fourier transform of Z given by

$$Z_T^{(3)}(\mathbf{P}, \mathbf{k}, \mathbf{r}_3) = \int d^3\rho_3' \int d^3r_{12}' \exp(-i2\mathbf{P}\cdot\boldsymbol{\varrho}_3')$$

$$\times \exp(-i\mathbf{k}\cdot\mathbf{r}_{12}') Z^{(3)}(\mathbf{r}_{12}', \boldsymbol{\varrho}_3', \mathbf{r}_3). \quad (4.16)$$

The coordinate $\mathbf{r}_3$ is unaffected, and this corresponds to keeping the particle 3 fixed instead of the center-of-mass. It should be noted that $\zeta_{\mathbf{k}\mathbf{P}}(\mathbf{r}_{12})$ actually depends also on the momentum of the third particle through the factor γ_1 [see Eq. (4.6)], but, as can be seen from Fig. 1, the function ζ does not vary much with γ for large γ_1, so that an average value may be used. Subject to this, Eq. (4.15) is still an exact representation of the operator $e^{-1}g_{12}$. Now, for $r_{12} < c$, we have

$$\zeta_{\mathbf{k}\mathbf{P}}(\mathbf{r}_{12}) = \exp(i\mathbf{k}\cdot\mathbf{r}_{12}),$$

so that

$$Z_g^{(3)}(\mathbf{r}_{12}, \boldsymbol{\varrho}_3, \mathbf{r}_3) = Z^{(3)}(\mathbf{r}_{12}, \boldsymbol{\varrho}_3, \mathbf{r}_3) \quad \text{for} \quad r_{12} < c. \quad (4.17)$$

For $r_{12} > c$, both the Day and Bethe approximations involve pulling the function $\zeta(\mathbf{r}_{12})$ outside the integral in Eq. (4.15), in some average sense. To justify this, we first note that in the reference approximation, the strongest dependence of $\zeta_{\mathbf{k},\mathbf{P}}(\mathbf{r}_{12})$ on the angles of $\mathbf{P}$, $\mathbf{k}$, and $\mathbf{r}_{12}$ is contained in $P_L(\hat{k}\cdot\hat{r}_{12})$, so that upon integration over d^3k, only the S-wave part $\zeta_{k,P}{}^0(r_{12})$ survives. Of course, the integrand also contains the Z function which depends on k as well. However, Kirson has shown that the conclusion, viz., that only the S-wave part of ζ matters, is nevertheless justified. One reason for this is that the components ζ^L for $L \neq 0$ are relatively small because the core does not have a

strong effect. There is only a very small dependence on the angle between P and k due to Pauli corrections etc. Further, as shown in Sec. 2 for $r_{12}>c$, the S-wave function $\zeta_{k,P}{}^0(r_{12})$ is nearly independent of k and P. The dependence on P arises through γ_1, to which $\zeta_{k,P}{}^0(r_{12})$ is not very sensitive, and the largest dependence on k arises because of matching the function at the core radius c, with the interior solution $j_0(kr)$. Thus it is reasonable to treat $\zeta_{k,P}{}^0(r_{12})/j_0(kc)=\zeta^D(r_{12})$ as essentially independent of k, and P, as long as these momenta are not large compared to c^{-1}. Hence we may write

$$Z_g{}^{(3)}(\mathbf{r}_{12},\boldsymbol{\varrho}_3,\mathbf{r}_3)$$

$$=\frac{8}{(2\pi)^6}\int d^3P\int d^3k\zeta_{\mathrm{k,P}}(\mathbf{r}_{12})\exp(2i\mathbf{P}\cdot\boldsymbol{\varrho}_3)Z_T{}^{(3)}(\mathbf{P},\mathbf{k},\mathbf{r}_3)$$

$$\simeq\frac{8}{(2\pi)^6}\zeta^D(r_{12})\int d^3P\int d^3k\exp(i\mathbf{k}\cdot\mathbf{c})$$

$$\times\exp(2i\mathbf{P}\cdot\boldsymbol{\varrho}_3)Z_T{}^{(3)}(\mathbf{P},\mathbf{k},\mathbf{r}_3)$$

$$\simeq\zeta^D(r_{12})Z^{(3)}(\mathbf{c},\boldsymbol{\varrho}_3,\mathbf{r}_3). \tag{4.18}$$

This is the Day approximation. The vector $\mathbf{c}$ is directed along $\mathbf{r}_{12}$, and $\zeta^D(r_{12})$, which is normalized to unity at the core radius, has to be evaluated for values of k and P at which the Fourier transform $Z_T{}^{(3)}$ is peaked. Kirson,[12] who explains the above approximation with greater care, shows that $Z_T{}^{(3)}$ is peaked around $k\simeq P\simeq 0.6/c$. This will be elaborated on later.

The Bethe approximation treats $\zeta_{k,P}{}^0(r_{12})/j_0(kr_{12})=\zeta^B(r_{12})$ as independent of k, P rather than $\zeta^D(r_{12})$. In this approximation,

$$Z_g{}^{(3)}(\mathbf{r}_{12},\boldsymbol{\varrho}_3,\mathbf{r}_3)\simeq[8/(2\pi)^6]\zeta^B(r_{12})\int d^3P\int d^3k$$

$$\times\exp(i\mathbf{k}\cdot\mathbf{r}_{12})\exp(2i\mathbf{P}\cdot\boldsymbol{\varrho}_3)Z_T{}^{(3)}(\mathbf{P},\mathbf{k},\mathbf{r}_3)$$

$$=\zeta^B(r_{12})Z^{(3)}(\mathbf{r}_{12},\boldsymbol{\varrho}_3,\mathbf{r}_3). \tag{4.19}$$

This is the Bethe approximation, which replaces $e^{-1}g_{12}$ simply by a multiplicative factor $\zeta^B(r_{12})$. We will first use the Bethe approximation which, because of the above simplicity, leads to an algebraic solution to the coupled equations (4.11) and reveals transparently some of the features of the three-body problem involved. We will then use the more accurate but more complicated Day approximation and discuss its merits over the Bethe approximation.

In the approximation of Eq. (4.19), the coupled equations (4.11) become

$$Z^{(3)}=\eta(\mathbf{r}_{13})+\eta(\mathbf{r}_{23})-\zeta^B(\mathbf{r}_{23})Z^{(1)}-\zeta^B(\mathbf{r}_{13})Z^{(2)}$$

$$\text{and cyclic permutations.} \tag{4.20}$$

Equations (4.20) can be solved algebraically for the Z's in terms of the η's and ζ's, which we know by solving the reference equation (2.4). We get

$$Z^{(3)}=\frac{\eta_{23}u_{23}+\eta_{13}u_{13}-\eta_{12}(u_{13}+u_{23}-2u_{13}u_{23})}{u_{23}u_{13}+u_{13}u_{12}+u_{12}u_{23}-2u_{12}u_{23}u_{13}}, \tag{4.21}$$

where

$$u_{ij}=1-\zeta_{ij}{}^B=1-\zeta^B(\mathbf{r}_{ij})$$

and

$$\eta_{ij}=\eta(\mathbf{r}_{ij}).$$

We can insert these $Z^{(i)}$ into the integral (4.12) for the three-body energy.

Take, for instance, diagrams of the type shown in Fig. 6. These diagrams, summed over l, m, n, give

$$W=\rho^2\int\eta(\mathbf{r}_{12})g(\mathbf{r}_{23})Z^{(1)}(\mathbf{r}_1\mathbf{r}_2\mathbf{r}_3)\,d\tau_1\,d\tau_2 \quad \text{per particle,} \tag{4.22}$$

where particle 3, instead of the center of mass, is kept fixed. Note that one of the Ω's in Eq. (4.12) is cancelled by integration over the coordinate of the fixed particle 3. The result (4.22) is proportional to ρ^2, as expected on physical grounds for three-body clusters.

Whereas we can evaluate $Z^{(1)}$ from Eq. (4.21) and integrate (4.22) for W, it is useful, as shown by Bethe, to study the solution in certain limiting cases using simplifying approximations to gain some insight into what is going on. Let us, as before, replace $\Phi=|lmn\rangle$ by unity since the hole state momenta are small. Let us also take $\eta(\mathbf{r}_{ij})$ and $\zeta^B(\mathbf{r}_{ij})$ to depend only on the magnitude of r_{ij}. This is reasonable, as explained before, since we are using averages over the momenta anyway and the angular averaging will pick out only the S-wave parts. (BBP show,[4] for instance, that η and ζ for $L\neq 0$ can be represented by a function of the type $e^{-\gamma r}/r$ outside the core with a somewhat larger value of γ than the true value.) In this approximation and in uniform nuclear matter, the functions g, η, and $Z^{(i)}$ all depend only on the relative separation distances r_{ij}, since no directions have been picked out in space.

Now take the case when all three particles are far apart, i.e., $r_{ij}\to\infty$. Then $\zeta^B(r_{ij})\to 0$ and $u(r_{ij})\to 1$. Thus,

$$Z^{(1)}\to\eta_{12}+\eta_{13} \tag{4.23}$$

and

$$W\to W_{\mathrm{III}}=\rho^2\int\eta(r_{12})g(r_{23})\{\eta(r_{12})+\eta(r_{13})\}\,d\tau_1\,d\tau_2. \tag{4.24}$$

It is easy to see that Eq. (4.24) is just the sum of the third-*order* direct diagrams in Fig. 3(a) and 3(b). Kohler[23] had obtained a similar form for the diagram 3(b). The fact that W becomes just the third-order

[23] H. S. Köhler, Ann. Phys. (N.Y.) 12, 444 (1961).

energy for large r_{ij} is reasonable since at these distances the potential is weak enough to give a good convergence order by order and the third order clearly dominates the three-body energy. To see the behavior for smaller values if r_{ij}, let us look at the case

$$r_{12}=r_{23}=r_{13}.$$

Then $u_{12}=u_{13}=u_{23}=u=1-\zeta$ and $\eta_{12}=\eta_{23}=\eta_{13}=\eta$. Thus,

$$Z^{(1)}=2\eta/(3-2u)=2\eta(1+2\zeta). \quad (4.25)$$

If the distances r_{ij} are very small (within the core radii), then $\zeta=1$ and

$$Z^{(1)}=2\eta/3. \quad (4.26)$$

This clearly corresponds to the very strong potential in the core region, and hence represents all orders of perturbation. This result is a third of Eq. (4.23) which represents only the third-order contribution. This diminution by a factor of 3 in the core region, in going from third order to all orders, may be partly understood thus: When two nucleons are within a core radius apart, the infinite core completely destroys the wave function in that region and leads to a large ζ and large energy. When three nucleons are all within each other's cores, an uncorrelated treatment will give three times this energy since three such pairs are involved. This is what happens in third order. In actuality however, we can do no more than destroy the wave function once when all the nucleons are close together, so that a fully correlated treatment (full three-body energy to all orders) will give only $\frac{1}{3}$ of the third-order energy. Actually, when all $r_{ij}<c$, this solution is exact, since under these conditions, $\zeta_{ij}=\eta_{ij}=e^{-1}g_{ij}=1$ so that the original coupled equations (4.11) become

$$Z^{(3)}=2+Z^{(2)}+Z^{(1)}.$$

However, when all $r_{ij}<c$, the three particles are in identical situations and hence by symmetry $Z^{(1)}=Z^{(2)}=Z^{(3)}=\frac{2}{3}$. This solution, simple and exact for all $r_{ij}<c$, should be remembered in the context of the Day approximation as well.

Finally, for small ζ, one can expand (4.25) as

$$Z^{(1)}=2\eta/(1+2\zeta)=2\eta-4\eta\zeta+8\eta\zeta^2-16\eta\zeta^3+\cdots. \quad (4.27)$$

This series represents the contribution of three-body diagrams, order by order. It is clearly not convergent for $\zeta>\frac{1}{2}$. For large interparticle separations, $\zeta\to 0$, and hence the series converges rapidly, so that a few lower order diagrams suffice for the pure long range part of the force. Within the hard core, however, $\zeta=1$ and the terms in the expansion (4.27) keep increasing although the whole series has a closed sum of $2\eta/3$. Even for any reasonable "soft" repulsive core, ζ is still a little greater than $\frac{1}{2}$ and the perturbation expansion above will not converge. (See, for instance, Sprung and Bhargava's work[8] using the Bressel potential[7] with only a finite core of about 650 MeV.)

Thus we see many of the anticipated features of the three-body problem in this simplified discussion. More exact results can, of course, be obtained from Eqs. (4.21) and (4.22). We note at this point that Eq. (4.24) may be written as[24]

$$W_{\mathrm{III}}=\rho^2\int g(r_{23})F_a(r_{23})\,d\tau_{23},$$

where

$$F_a(r_{23})=\int \eta(r_{12})\{\eta(r_{12})+\eta(r_{13})\}\,d\tau_1. \quad (4.28)$$

Similarly, for the full three-body energy

$$W=\rho^2\int g(r_{23})F_1(r_{23})\,d\tau_{23},$$

where

$$F_1(r_{23})=\int \eta(r_{12})Z^{(1)}(r_{12},r_{23},r_{13})\,d\tau_1. \quad (4.29)$$

We will give graphs of the functions F_a, F_1, using the more accurate Day approximation for the $Z^{(i)}$, which we will outline now.

Day's Approximation

Day approximates the action of the operator $e^{-1}g_{ij}$ by Eq. (4.18) as compared to the simpler multiplicative approximation by Bethe in Eq. (4.19). It is clear that Day retains more of the operative character of $e^{-1}g_{ij}$, and, as we shall see, his resulting solutions for the $Z^{(1)}$ are considerably better. As the $Z^{(1)}$ are functions only of the interparticle distances, we can rewrite the Day approximation (4.18) as

$$e^{-1}g_{12}Z^{(3)}(r_{12},r_{23},r_{13})=Z_g^{(3)}(r_{12},r_{23},r_{13}),$$
$$=\zeta^D(r_{12})Z^{(3)}(c,r_{23}',r_{13}'), \quad (4.30)$$

where r_{23}' and r_{13}' correspond to the coordinates $\mathbf{c}$, ϱ_3,

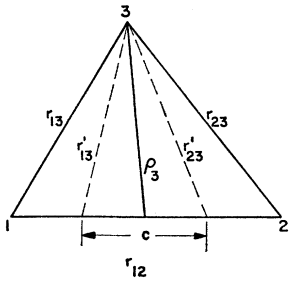

FIG. 9. Triangle formed by the three particles in coordinate space.

[24] All these formulas are valid only if g may be written as a function of r_{23} alone. For a more general treatment see Secs. 5 and 6.

and $\mathbf{r}_3$ in the Eq. (4.18), and their meaning can be read from Fig. 9. The Day approximation thus differs from that of Bethe, in that it "shrinks" the triangle of the particles in addition to multiplying by $\zeta^D(r_{12})$. Note that for $r_{12}<c$, $Z_0^{(3)}=Z^{(3)}$ [Eq. (4.17)] and $\zeta^D(r_{12})\simeq 1$.

Substituting (4.30) into the coupled equations (4.11), we get,

$$Z^{(3)}(r_{12}, r_{23}, r_{13}) = \eta(r_{23})+\eta(r_{13})-\zeta^D(r_{23}) \begin{cases} Z^{(1)}(r_{12}, r_{23}, r_{13}) & \text{if } r_{23}<c \\ Z^{(1)}(r_{12}', c, r_{13}') & \text{if } r_{23}>c \end{cases} - \zeta^D(r_{13}) \begin{cases} Z^{(2)}(r_{12}r_{23}r_{13}) & \text{if } r_{13}<c \\ Z^{(2)}(r_{12}', r_{23}', c) & \text{if } r_{23}>c \end{cases}. \tag{4.31}$$

These equations correspond to Eq. (4.20) of the Bethe approximation and, unlike the latter, cannot be solved algebraically, since $Z^{(3)}$ at one set of points is coupled to $Z^{(2)}$ and $Z^{(1)}$ at other points on the "reduced triangle." Of course, if all $r_{ij}<c$, then the solution is $Z^{(1)}=\frac{2}{3}\eta$. Similarly, if only $r_{12}>c$, then r_{13}' and r_{23}' are necessarily less than c, so that $Z^{(1)}(c, r_{23}', r_{13}')=\frac{2}{3}\eta$, and this again leads to an analytical solution of (4.31). But, for the general case where at least two of the r_{ij} are greater than c, one has to resort to a numerical method. The method involves substituting for the $Z^{(1)}(r_{12}', c, r_{13}')$ and $Z^{(2)}(r_{12}', r_{23}', c)$ in Eq. (4.31) from the other two coupled equations, which leads to points on a smaller triangle. If this is repeated successively, you eventually reach (in general) a triangle where at least two of $r_{ij}<c$, when the solution is known. Day has calculated this numerical solution for several values of r_{ij}. However, the method does not work for some instances such as when all three particles are collinear, in which case you never reach a stage when two of the distances are less than c. In the more general case, the numerical solution is laborious.

Consequently, Day has suggested that Eqs. (4.31) be replaced by an approximate form which is amenable to an analytic solution. The wave-function defects $Z^{(i)}$ are large only when the $r_{ij}\sim c$, and all the ζ's and η's drop off rapidly for $r_{ij}>c$. But if r_{12} is not much larger than c, then $r_{13}'\sim r_{13}$ and $r_{23}'\sim r_{23}$. Thus, one might try to replace Eq. (4.31) by

$$Z^{(3)}(r_{12}, r_{23}, r_{13}) = \eta(r_{23})+\eta(r_{13})-\zeta^D(r_{23}) \begin{cases} Z^{(1)}(r_{12}, r_{23}, r_{13}) & \text{if } r_{23}<c \\ Z^{(1)}(r_{12}, c, r_{13}) & \text{if } r_{23}>c \end{cases} - \zeta^D(r_{13}) \begin{cases} Z^{(2)}(r_{12}, r_{23}, r_{13}) & \text{if } r_{13}<c \\ Z^{(2)}(r_{12}, r_{23}, c) & \text{if } r_{13}>c \end{cases}. \tag{4.32}$$

These equations are amenable to an analytic solution. This simply involves substituting for $Z^{(1)}$ and $Z^{(2)}$ from the other two coupled equations when you get two of the r_{ij} to be equal. One can then exploit symmetry properties such as $Z^{(3)}(c, r_{23}, c)=Z^{(2)}(c, r_{23}, c)$ and $Z^{(1)}(c, c, r)=Z^{(1)}(r, c, c)$ to solve the set of three equations implied in (4.32). The result is

$$\begin{aligned} Z^{(1)}(r_{12}, r_{23}, r_{13}) &= \eta_{12}(1-\zeta_{13}+\tfrac{1}{2}\zeta_{13}\zeta_{23}) \\ &+\eta_{13}(1-\zeta_{12}+\tfrac{1}{2}\zeta_{12}\zeta_{23})-\eta_{23}(\zeta_{12}+\zeta_{13}+\zeta_{12}\zeta_{13}) \\ &+[\zeta_{12}\zeta_{13}+\tfrac{1}{2}(\zeta_{12}+\zeta_{13})\zeta_{23}-\tfrac{4}{3}\zeta_{12}\zeta_{13}\zeta_{23}], \end{aligned} \tag{4.33}$$

with $\eta_{ij}=\eta(r_{ij})$ and $\zeta_{ij}=\zeta^D(r_{ij})$.

This is Day's analytic solution to (4.32). Day finds[21] that it agrees very well with the numerical solution to his original equations (4.31). Further, Kirson[12] finds that when the analytic solution (4.33) is substituted into the right-hand side of (4.31), the resulting iterated solution for $Z^{(3)}(r_{12}, r_{23}, r_{13})$ is very close to the analytic solution. Two of Kirson's graphs comparing the analytic solution (4.33) and its first iteration are given in Fig. 10. Since the analytic solution agrees very closely with its first iterate and with the numerical solution to the more exact equations (4.31) evaluated by Day for several sets of values of r_{ij}, and since (4.31) itself is only an approximation, we will use Eq. (4.33) for the $Z^{(i)}$.

This analytic solution by Day is considerably better than the simpler solution (4.21) for the $Z^{(i)}$. First of all, the underlying approximation for the operator $e^{-1}g_{ij}$ in Eq. (4.18) is more accurate than the corresponding Bethe approximation in Eq. (4.19). Secondly, the Bethe solution has drastic discontinuities which occur sometimes when one of the r_{ij} equals c. This may be partly understood by considering the solution (4.21) when all $r_{ij}\to c^+$. Then the $u_{ij}=1-\zeta_{ij}^B$ tend to vanish and the solution approaches the indeterminate form

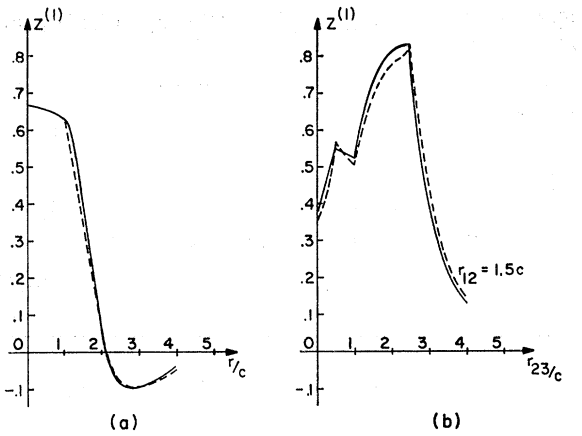

FIG. 10. Two graphs due to Kirson[12] comparing Day's analytical solution (solid line) and its first iterate (dashed line). Graph (a) is for all $r_{ij}=r$ while graph (b) has $r_{13}=|r_{23}-r_{12}|$ and $r_{12}=1.5c$.

0/0, whereas when all $r_{ij}<c$, we know the result to be $Z^{(i)}=\frac{2}{3}$. When r_{23} and r_{13} are less than c, the Bethe solution gives

$$Z^{(3)}=(1-\eta_{12})/2u_{12}. \tag{4.34}$$

If now r_{12} approaches c from outside, the above solution is highly sensitive to the exact behavior of η_{12} and $\zeta_{12}{}^{B}$ near the core, whereas for $r_{12}<c$, it is equal to $\frac{2}{3}$. There are no such discontinuities in the Day solution.

A comparison of the Day and Bethe solutions is given in Fig. 11. Of course, the three-body energy and the function F_a and F_1 involve *integrals* of the $Z^{(i)}$ and consequently the two solutions give comparable results since the discontinuities do not matter here. But Dahlblom,[25] doing the corresponding calculation for tensor forces (see Sec. 6), found that the Bethe procedure led to great difficulties while the Day method was straightforward. With central forces also the Day solution is clearly more accurate. This is especially clear from Kirson's work: If the solution (4.21) is used on the right-hand side of (4.31), the resulting iterated solution is completely different, in contrast to the behavior of the Day solution, Fig. 10.

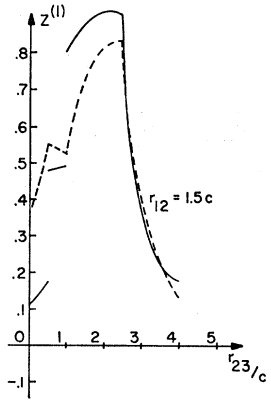

FIG. 11. A comparison of the Day and Bethe solutions, exhibiting the strong discontinuities of the latter (solid line) as compared to the former (dashed line). The graph is drawn for $r_{12}=1.5c$, $r_{13}=|r_{23}-r_{12}|$.

[25] T. Dahlblom, Nucl. Phys. (to be published).

It should be mentioned at this stage that having obtained the $Z^{(i)}$ by the above methods, Kirson evaluates their momentum transform and finds it peaked at k, $P\simeq 0.6/c$. This was mentioned earlier in connection with Eqs. (4.18) and (4.19), where the function ζ had to be factored out of the integral for the $Z_g{}^{(1)}$. This factoring was justified only if the ζ was relatively independent of k, P, which is true only if they are less than $1/c$. It is therefore gratifying that the momentum dependence of the $Z^{(1)}$ conforms to this requirement. Further, Kirson finds that if k, $P\simeq 0.6/c$ are used as input in Eq. (4.19), the resulting $Z^{(1)}$ give an output momentum dependence which agrees well with the input.

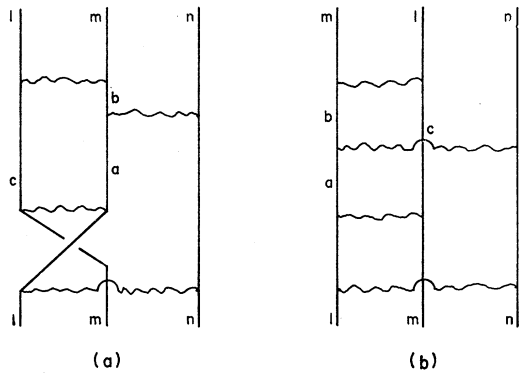

FIG. 12. An exchange diagram represented in two equivalent ways.

This completes our discussion of the evaluation of the three-body wave-function defects $Z^{(1)}$. The Day solution (4.33) may be used for evaluating the function F_a or the more complicated expressions derived in Secs. 5 and 6 and the three-body energy as defined by Eqs. (4.29) and (4.12), respectively. We will quote the results after discussing exchange diagrams.

Exchange Diagrams

The problem of exchange diagrams may seem complicated inasmuch as for every direct diagram you can exchange any of the interactions, or "rungs of the ladder" in the diagram. However, as is illustrated in the example in Fig. 12, when you exchange an intermediate interaction, the resulting diagram can be redrawn so that it looks like a direct diagram with two of the final momenta **l** and **m** exchanged, as compared to the initial ordering of the three momenta. Thus Fig. 12(a) and 12(b) are equivalent. It is clear therefore that no matter how many of the interactions are exchanged, the result would simply amount to permuting the final momenta **l**, **m**, and **n**. Thus, all direct and

exchange diagrams would be contained in $\langle lmn \mid T \mid lmn\rangle$, $\langle mln \mid T \mid lmn\rangle$, $\langle lnm \mid T \mid lmn\rangle$, $\langle nml \mid T \mid lmn\rangle$, $\langle mnl \mid T \mid lmn\rangle$, and $\langle nlm \mid T \mid lmn\rangle$. The exchange diagrams, however, carry additional statistical weights as compared to the direct diagrams, if one uses spin–isospin-independent forces.[14] For such forces, each particle retains its spin–isospin values, and hence all states on a given vertical line in the direct diagram have the same value of s_z and τ_z, although any two vertical lines may have different spin and isospin components. However, for an exchange diagram such as the ones in Fig. 12, both the states **l** and **m** must have the same spin–isospin since a particle from each of these states goes into the other. Thus, the number of allowed states, and hence the contribution to the energy, is reduced by a factor of 4. In addition, if these diagrams are drawn in the Goldstone Convention, it can be seen that Fig. 12 corresponds to only two nucleon loops, unlike the three in a direct diagram. Consequently, according to the Goldstone rule, there is an additional minus sign associated with Fig. 12, and altogether, therefore, it is multiplied by $-\frac{1}{4}$ due to the above arguments. Similarly, when all three nucleons interchange momenta, as in $\langle mnl \mid T \mid lmn\rangle$, there is a multiplicative factor of $+1/16$ since now all three nucleons must have the same s_z and τ_z, with only one nucleon loop altogether. These arguments clearly have to be modified for tensor forces.

But for these statistical factors, the matrix elements $\langle lmn \mid T \mid lmn\rangle$ and any one of its exchanges, say $\langle lnm \mid T \mid lmn\rangle$, are not very different. Compare, for instance, the two diagrams in Fig. 13 which are corresponding terms belonging to $\langle lmn \mid T \mid lmn\rangle$ and $\langle lnm \mid T \mid lmn\rangle$, respectively. For every set of intermediate momenta in Fig. 13(a) there is a term with the same set in Fig. 13(b). The only difference is in the final interaction. The final interaction has different matrix elements for the two cases, since the momentum transfer in the two cases is different by $\mathbf{q}=\mathbf{m}-\mathbf{n}$. But

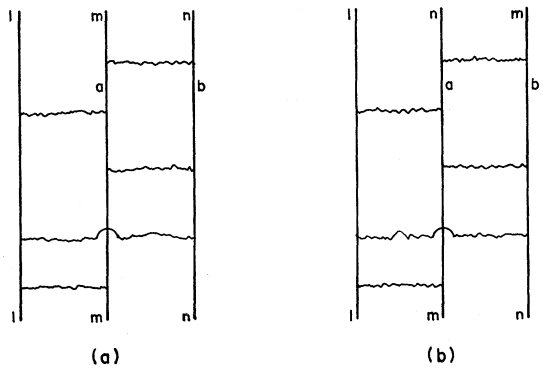

FIG 13. Comparison of a direct diagram belonging to $\langle lmn \mid T \mid lmn\rangle$ and an exchange diagram belonging to $\langle lnm \mid T \mid lmn\rangle$.

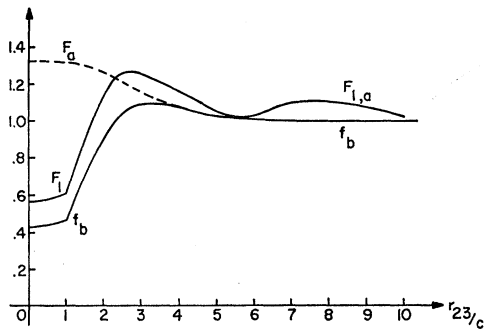

FIG. 14. A graph of the functions F_a, F_1, and f_b defined in (4.28), (4.29), for a standard hard core potential.[12]

since **m** and **n** are holes, the average value of $qc=(1.2)^{1/2}k_F c\simeq 0.6$, and it was shown[14] in the context of third-order diagrams that the resulting difference is only a factor of about $\frac{1}{6}q^2c^2$, i.e., about 6%. Therefore, up to a few percent, the direct and exchange matrix elements of T are equal.

It was also shown by Bethe[6] that, in the approximation of neglecting q^2c^2, the inclusion of all exchange terms amounts to using even angular momentum contributions only. This has no effect for a Serber-type attractive force, which acts only on even L states anyway, but it cuts down the repulsive core effect to only the even L states, supporting such an assumption that had been made by Brueckner and Gammel[26] in their g-matrix calculations.

Several calculations have been made, using the above method for evaluating the three-body energy by Sprung, Bhargava, and Dahlblom,[27] and by Kirson.[12] Kirson uses the full standard hard-core potential, including the short- and long-range parts, to obtain an energy of -5.15 MeV for the three-body clusters. His curves for the functions $F_1(r_{23})$, $F_a(r_{23})$, and $f_b(r_{23})$ defined earlier are depicted in Fig. 14. As anticipated, for large r_{23}/c, all three functions approach the same value, 1. At small distances, F_1 is about a third of F_a, as expected from Eq. (4.26). The curves have been drawn to a scale where $F_0(r_{23})$, the corresponding function for just the third-order bubble diagram, is taken to be unity.

The diminution from -38.35 to -5.15 MeV in going from the two-body to the three-body contribution indicates that our hopes of convergence in powers of density appear justified. It will be seen in Sec. 7 that the long-range part v_l contributes most of the -5 MeV in the three-body energy, and that the energy for just the short range part is a small positive amount. We therefore can expect a four-body energy of much less than 1 MeV for v_s. It will be shown in Sec. 7 that most of

[26] K. A. Brueckner and J. L. Gammel, Phys. Rev. **109**, 1023 (1958).

[27] D. W. L. Sprung, P. C. Bhargava, and T. Dahlblom, Phys. Letters **21**, 538 (1966).

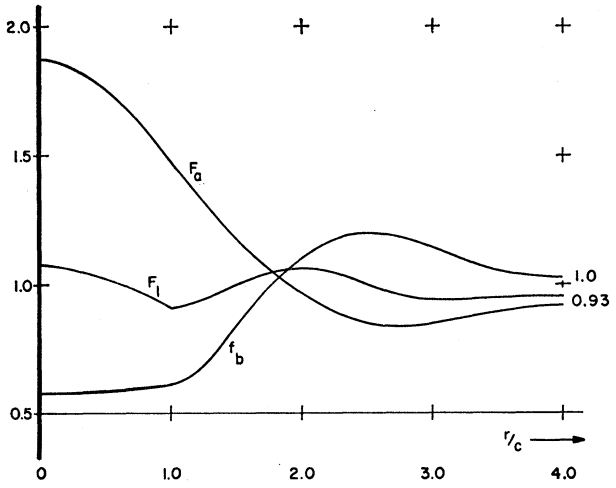

FIG. 15. The functions F_a, F_1, and f_b using the Reid potential[7] for triplet states.

the higher order effects of v_l can, on the other hand, be absorbed in the single-particle potential energy $U(b)$.

A more recent calculation by Dahlblom of the functions F_1, F_a, and f_b is given in Fig. 15. This calculation uses the Reid potential[7] of 1965 for triplet states, which has a hard core of about 0.52 F and consequently a stronger attraction outside.

5. EFFECT OF THE MOMENTUM DEPENDENCE OF THE g MATRIX

We now proceed to a systematic evaluation of the three-body energy. In particular, we shall take into account the momentum dependence of g which was mentioned below Eq. (4.14) but was then ignored in the remainder of Sec. 4. To do this, we must go back to the fundamental Eq. (4.12), line before the last. From this, or from Fig. 16 (which is just Fig. 6 with different features emphasized), we find, in slightly different notation,

$$W_3(K_0)=\int dK_1\,dK_2\langle K_0\mid\hat{\eta}_{12}\mid K_1\rangle \times\langle K_1\mid\hat{g}_{23}\mid K_2\rangle\langle K_2\mid\hat{Z}^{(1)}\mid K_0\rangle. \quad (5.1)$$

Here each K_i stands for the momenta of all three particles; specifically K_0 refers to the initial and the others to the two intermediate states. The final state is of course identical with the initial. The η, g, and Z are operators and have therefore been denoted by a $\wedge$. The first operator represents

$$\hat{\eta}_{12}=\hat{g}_{12}(Q/e), \quad (5.2)$$

i.e., the last interaction and the preceding propagator. The last interaction is separated from the rest in this manner because the e here corresponds to the excitation of 2 particles while "earlier" propagators correspond to excitation of 3 particles, as explained in (4.5), (4.6). Equation (5.1) is somewhat more general than (4.12) in that the momenta in initial and final state are not yet put to zero. Following Kirson and the discussion in Sec. 4, we shall assume that the three-body wave-function operator $Z^{(1)}$, operating on the unperturbed wave function $\mid K_0\rangle=\Phi$, may be written as

$$\hat{Z}^{(1)}\mid K_0\rangle=Z^{(1)}(r_{12},r_{23},r_{31})\Phi(K_0), \quad (5.3)$$

where $\Phi(K_0)$ is the unperturbed wave function (product of three plane waves) and the function $Z^{(1)}$ depends only on the distances between the three particles, not on the directions of the vectors $\mathbf{r}_{12}$ etc.

The problem then is the matrix element of g_{23}. This quantity depends appreciably on the relative momentum of particles 2 and 3 in state K_1. To see this, we write

$$\hat{g}_{23}\mid K_1\rangle=e\hat{\xi}_{23}\mid K_1\rangle, \quad (5.4)$$

where $\hat{\xi}_{23}$ is the two-body defect function as defined in Sec. 3, and the operator e may be written in the reference spectrum approximation

$$e=\gamma^2-\nabla_{23}^2. \quad (5.5)$$

As is shown in BBP, γ increases with increasing excitation of the state K_1. Therefore, just *because* ζ is very insensitive to K_1 (Ref. 6, p. 809), g is very sensitive: it increases rapidly with increasing energy. This is particularly true for the contribution from inside the core; we have

$$\hat{\xi}_{23}\mid K_1\rangle=\mid K_1\rangle, \qquad r_{23}<c, \quad (5.6)$$

$$\hat{g}_{23}\mid K_1\rangle=(k_{23}^2+\gamma^2)\mid K_1\rangle, \qquad \text{if } r_{23}<c, \quad (5.7)$$

where k_{23} is the relative momentum of particles 2 and 3 in state K_1. The contribution from the core surface [Ref. 4, Eq. (5.28)] is less sensitive to the energy of state K_1, and that from the long-range, attractive

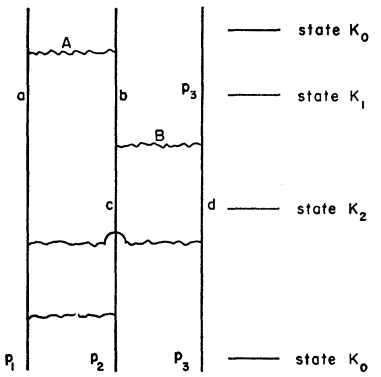

FIG. 16. A three-body diagram. K_0, K_1, and K_2 each stand for the momenta of all thre particles at the respective stages.

forces is insensitive, viz.,

$$\hat{g}_{23} \mid K_1\rangle \approx v(r_{23}) \mid K_1\rangle, \qquad r_{23} \gg c. \tag{5.8}$$

A simple approximation was made by Kirson: He replaced g by its value for the *average* momentum k_{23} of the interacting particles. He justified this approximation by his finding that the distribution of the momentum k_{23} in state K_1 is sharply peaked around its average value of about $0.6/c$ [cf. this paper above (4.19)]. Hence Kirson puts

$$\hat{g}_{23} \mid K_1\rangle = g_{23}(k_{23\mathrm{Av}}, r_{23})\Phi(K_1), \tag{5.9}$$

where $\Phi(K_1)$ is the product of three plane waves corresponding to the momenta in state K_1, and g_{23} is simply a function of r_{23}. If this is assumed, the integration over K_1 and K_2 in (5.1) can be done immediately and gives

$$W_3(K_0) = \langle K_0 \mid \eta^*(r_{12})\, g_{23}^*(r_{23})\, Z^{(1)}(r_{12}, r_{23}, r_{31}) \mid K_0\rangle, \tag{5.10}$$

substantially equivalent to (4.12).

Because of the considerable sensitivity of g_{23} to k_{23}, the choice of $k_{23\mathrm{Av}}$ in the Kirson approximation is rather critical, and it is not clear what criteria to use. Bethe has given a more general solution. He writes

$$\hat{g}_{23} \mid K_1\rangle = g_{Pk}(\mathbf{r}_{23})\Phi(K_1), \tag{5.11}$$

where P and k are, respectively, the average and the relative momentum of particles 2 and 3 in the state K_1. The function g depends on both these parameters, and it is therefore not possible to effect "closure" with respect to K_1. However, closure *is* possible with respect to K_2, and leads to the result

$$W^3(K_0) = \pi^{-3} \int d^3k \langle K_0 \mid \eta_{12} \mid K_1\rangle\langle K_1 \mid g^* Z^{(1)} \mid K_0\rangle, \tag{5.12}$$

$$\langle K_1 \mid g^* Z^{(1)} \mid K_0\rangle = \int d^3r_{12} \int d^3r_{23} g^*_{Pk}(\mathbf{r}_{23}) Z^{(1)}(r_{12}, r_{23}, r_{31}) \exp i(\mathbf{p}_3 - \mathbf{p}_2 + 2\mathbf{k})\cdot\mathbf{r}_{12}, \tag{5.13}$$

$$\langle K_0 \mid \eta \mid K_1\rangle = \int d^3r_{12} \eta^*(r_{12}) \exp i(\mathbf{p}_3 - \mathbf{p}_2 + 2\mathbf{k})\cdot\mathbf{r}_{21}. \tag{5.14}$$

Here $\mathbf{p}_1$, $\mathbf{p}_2$, $\mathbf{p}_3$ are the initial momenta of the three particles in state K_0, and $2\mathbf{k}$, as in (5.11), is the difference between the momenta of particles 2 and 3 in the intermediate state K_1.

Two alternatives are now open. One is to calculate and use the exact expression for $g_{Pk}(\mathbf{r}_{23})$; then no further simplification of (5.13) seems possible. The other is to find a manageable approximation to the dependence of g on P and k; this is probably sufficient because the entire three-body correlation contributes less than 20% to the total potential energy of nuclear matter. Such an approximation is suggested by (5.7) and (5.8), together with (4.5) and the discussion of BBP Sec. 7. The state K_1 is characterized by the excitation of only two particles, 1 and 2. In this case, if k_b denotes the momentum of particle 2, (4.5) shows that in (5.7)

$$k_{23} \equiv k \simeq \tfrac{1}{2}k_b$$

and

$$k_{23}^2 + \gamma^2 = k_b^2 \tag{5.15}$$

neglecting k_F^2 compared with k_b^2. Then, considering the two components (5.7) and (5.8) of g and assuming that the contribution from the core surface has an intermediate behavior, it is reasonable to set

$$g_{Pk}(r_{23}) = g_1(r_{23}) + k^2 g_2(r_{23}). \tag{5.16}$$

Here we have used both equations (5.15).

Before (5.16) can be used, it is still necessary to make assumptions about the nuclear force, as follows:

(1) An *ordinary* (nonexchange, central) force between the nucleons, which may include a repulsive core, can be represented quite well by (5.16). In evaluating g_1 and g_2, the definition of g should be remembered:

$$g_{Pk}(\mathbf{r})\phi(\mathbf{r}) = v(r)\psi_{Pk}(\mathbf{r}), \tag{5.17}$$

where $\phi = \exp(i\mathbf{k}\cdot\mathbf{r})$ and $\psi = \phi - \zeta$ is the two-particle wave function with interaction. In practice it is probably best to calculate g_{Pk} by explicit integration of the Schrödinger equation for several values of k on both sides of the most probable value of k determined by Kirson ($k = 0.6/c$), and then to deduce g_1 and g_2 from these. Such a program has been carried out by Dahlblom.[25]

If (5.16) is accepted, integration of (5.13) over K_1 is straightforward for g_1.[28] The factor k^2 multiplying g_2, on the other hand, can be combined with the η matrix element, if we assume

$$|\, p_3 - p_2 \,| \ll 2k \tag{5.18}$$

[28] The asymmetry in K_1 and K_2 is arbitrary. It would be equally possible to let g depend on the momenta in state K_2; then closure with respect to K_1 could be accomplished. However, K_1 is more simply defined by the two-body function η_1 while K_2 requires analysis of the complicated 3-body function Z.

which is generally a good approximation since p_3 and p_2 are $<k_F$. The result is then[29]

$$W_3(K_0)=\int d^3r_{21}\,d^3r_{23}[\eta^*(r_{12})g_1^*(r_{23}) -\tfrac{1}{4}\nabla^2\eta^*(r_{12})g_2^*(r_{23})]Z^{(1)}(r_{12},r_{23},r_{31}). \quad (5.19)$$

Since both η and $Z^{(1)}$ are essentially independent of the momenta $\mathbf{p}_1$, $\mathbf{p}_3$, $\mathbf{p}_3$, this result may simply be multiplied by ρ^2 to give the energy per particle. The effect of nonvanishing momenta $\mathbf{p}_1$, $\mathbf{p}_2$, $\mathbf{p}_3$ can be treated approximately, using the method of Kirson.[12]

Equation (5.19) can be further simplified. Since g depends only on r_{23}, we can integrate over the position of particle 1, i.e., over $\mathbf{r}_{12}$, keeping r_{23} fixed. This yields

$$F_1(r_{23})=\int d^3r_{12}\eta^*(r_{12})Z^{(1)}(r_{12},r_{23},r_{31}), \quad (5.20)$$

$$F_2(r_{23})=-\tfrac{1}{4}\int d^3r_{12}(\nabla^2\eta^*(r_{12}))Z^{(1)}(r_{12},r_{23},r_{31}), \quad (5.21)$$

$$W_3(K_0)=\int d^3r_{23}[g_1^*(r_{23})F_1(r_{23})+g_2^*(r_{23})F_2(r_{23})]. \quad (5.22)$$

The function F_1 is identical with the F introduced in Ref. 6, Eq. (5.1), which was there shown to be small if r_{23} is inside the core and to increase rapidly (by about a factor 3) outside. The other correlation function F_2 was introduced in Ref. 29.

Dahlblom[25] has calculated F_1 and F_2 for the Reid, hard-core potential of 1965. The result is given in Fig. 17. Note that F_1 is almost independent of r while F_2 is much smaller at small than at large r. This suppresses the strong part of the core repulsion which is proportional to k^2.

(2) *A more realistic nuclear force* may be considered, in first approximation, as a superposition of two parts, (a) a Serber force

$$\hat{v}_e\psi(\mathbf{r})=\tfrac{1}{2}v_e(r)[\psi(\mathbf{r})+\psi(-\mathbf{r})] \quad (5.23)$$

and (b) an additional attractive force acting in the S state only

$$v_s(\mathbf{r})=v_s(r)\psi_0(r), \quad (5.24)$$

with ψ_0 denoting the $L=0$ component of the wave function (subscripts e for even L, S for S state). The Serber force acts in all two-body states of even L, with $L=0$ and 2 being the only important ones, while the need for the force (b) arises from the observed fact[30,31] that the nucleon–nucleon potential is more attractive in the ^1S than in the ^1D state.

(a) If it is assumed that the Serber force v_e acts only for large r, we can proceed as in (5.8) and can replace $\psi(\mathbf{r})$ by the unperturbed wave function $\phi(\mathbf{r})=\exp(i\mathbf{k}\cdot\mathbf{r})$. In this case, (5.22) is replaced by[29]

$$W_{3e}(K_0)=\tfrac{1}{2}\int d^3r_{12}\,d^3r_{23}[\eta^*(r_{12})+\eta^*(r_{13})] \times v_e(r_{23})Z^{(1)}(r_{12},r_{13},r_{23}). \quad (5.25)$$

Here the first term $\eta(r_{12})$ arises from the "direct" term in the Serber force, $\psi(\mathbf{r})$ in (5.23), while $\eta(r_{13})$ arises from the exchange term, $\psi(-\mathbf{r})$. But $Z^{(1)}$ is clearly symmetric in r_{12} and r_{13}; therefore the two terms in the bracket of (5.23) give equal contributions, and the Serber force gives exactly the same result as an ordinary force. This is in accord with the discussion at the end of Sec. 4.

It is then possible to drop the assumption that v_s acts only at long distances r, and to assume instead

$$\hat{v}_e\psi(r)=\tfrac{1}{2}[g_{e1}(r)+k^2g_{e2}(r)][\phi(\mathbf{r})+\phi(-\mathbf{r})] \quad (5.26)$$

in analogy with (5.16). The result is exactly (5.22).

(b) The S-state force (5.24) is somewhat more complicated. Assuming, again in analogy with (5.16),

$$v_s(r)\psi_0(r)=[g_{s1}(r)+k^2g_{s2}(r)]\phi_0(r),$$
$$\phi_0(r)=j_0(kr), \quad (5.27)$$

Bethe obtains

$$W_{3s}(K_0)=\int d^3r_{23}[g_{s1}(r_{23})F_{s1}(r_{23})+g_{s2}(r_{23})F_{s2}(r_{23})], \quad (5.28)$$

$$F_{s1}(r_{23})=r_{23}^{-1}\int d^3r_{12}R^{-1}[\chi(R-\tfrac{1}{2}r_{23})-\chi(R+\tfrac{1}{2}r_{23})]Z^{(1)}, \quad (5.29)$$

$$F_{s2}(r_{23})=(4r_{23})^{-1}\int d^3r_{12}R^{-1} \times[\omega(R-\tfrac{1}{2}r_{23})-\omega(R+\tfrac{1}{2}r_{23})]Z^{(1)}, \quad (5.30)$$

$$R=\tfrac{1}{2}\,|\,\mathbf{r}_{12}+\mathbf{r}_{13}\,|, \qquad R^2=\tfrac{1}{2}(r_{12}^2+r_{13}^2)-\tfrac{1}{4}r_{23}^2,$$
$$\chi(x)=\int_x^\infty \eta(y)\,y\,dy,$$
$$\omega(x)=\eta(x)+x(d\eta/dx). \quad (5.31)$$

[29] H. A. Bethe, Phys. Rev. (to be published).

[30] P. Noyes, Conference on Nuclear Forces and the Few-Nucleon Problem (London, 1959); P. Noyes and T. Osborn (private communication, 1965).

[31] R. Reid, Cornell University thesis (1967); Phys. Rev. (to be published).

(3) *The tensor force* between nucleons 2 and 3 is conveniently replaced by the central force which results from it[32] in second-order perturbation theory. This force depends slightly on k, so that it should be a good approximation to write

$$\hat{g}_T\phi(\mathbf{r}) = (g_{T1}(r) + k^2 g_{T2}(r))\phi(\mathbf{r}), \qquad (5.32)$$

with g_{T1} attractive and g_{T2} repulsive. Thereby the tensor force is reduced to the same form as the other parts.

Summary. The total nuclear force may be well represented as a sum of an ordinary, a Serber, an S state, and a tensor force. The ordinary force may be chosen to include the effect of the repulsive force in the ^1P state and the repulsive core. All terms except the s-state force reduce to a result of the type (5.20)–(5.22), the s-state force gives (5.28)–(5.32).

Calculation. Dahlblom[25] has calculated the 3-body energy for the Reid, hard-core potential of 1965, and found +1.1 MeV. This is in contrast to earlier estimates of about −5 MeV by Kirson.[12] The change is partly due to the very flat function F_1 of Dahlblom, see Figs. 15 and 17, which is in contrast to Kirson's F_1, Fig. 14. Thus for Kirson the core repulsion was largely suppressed, for Dahlblom it is not. Part of the change is due to a misinterpretation of the theory in Kirson's paper (through no fault of his), see Appendix, which has been corrected by Dahlblom.

6. TENSOR FORCES

The theories of Bethe,[6] Day,[21] and Kirson[12] assume that the initial and final interactions in the three-particle ladder involve central forces, including a repulsive core. Dahlblom[25] has treated the case of a tensor force in the initial and final interaction, with central forces in all intermediate interactions. He assumes that the initial and final particle momenta are zero. Then the force in the ^3S-state modifies the two-particle function $\phi=1$ into

$$\psi = \phi - \eta^c(r) - \eta^T S_{12}, \qquad (6.1)$$

where η^c is the s-state defect function, previously called η in Secs. 4 and 5, while the last term is the D-state which is introduced by the tensor force. S_{12} is the usual tensor operator

$$S_{12} = 3\boldsymbol{\sigma}_1\cdot\hat{\mathbf{r}}\boldsymbol{\sigma}_2\cdot\hat{\mathbf{r}} - \boldsymbol{\sigma}_1\cdot\boldsymbol{\sigma}_2, \qquad (6.2)$$

with $\hat{\mathbf{r}}$ a unit vector in the direction $\mathbf{r}$. The contribution of the tensor force to the three-body energy is written (apart from a numerical factor)

$$W_T = \int \eta_{12}{}^T g_{23} Z^{(1)T}. \qquad (6.3)$$

Because of the spin operators in S_{12}, W_T is not symmetric in particles 2 and 3, in contrast to (4.33). Using otherwise Day's approximation, Dahlblom finds

$$\begin{aligned} Z^{(1)T} = {} & \eta_{12}{}^T[1-\zeta_{13}+\tfrac{1}{2}\zeta_{13}\zeta_{23}] \\ & -\tfrac{1}{2}P_2(\hat{\mathbf{r}}_{12}\cdot\hat{\mathbf{r}}_{13})\eta_{13}{}^T[1-\zeta_{12}+\tfrac{1}{2}\zeta_{12}\zeta_{23}] \\ & -\tfrac{1}{2}P_2(\hat{\mathbf{r}}_{12}\cdot\hat{\mathbf{r}}_{23})\eta_{23}{}^T[\zeta_{12}\zeta_{13}-\zeta_{12}-\zeta_{13}]. \end{aligned} \qquad (6.4)$$

In this expression, ζ is the wave-function defect due to central forces in an intermediate state, the same as in (4.33). P_2 is the second Legendre polynomial, and $\hat{\mathbf{r}}_{12}\hat{\mathbf{r}}_{13}$ is the cosine of the angle between the vectors named; this can be expressed in terms of the distances r_{12}, r_{13}, r_{23}. Equation (6.4) contains no counterpart to the last term in (4.33) which arose there from the Z inside the repulsive core. The tensor force inside the core is zero, hence this term is absent in (6.4). Since $V_T=0$ for $r<c$, the function η^T rises only slowly outside the core, (see the curve $u_{21}{}^{(0)}$ in Ref. 4, Fig. 13). On the other hand, ζ drops rapidly for $r>c$ (see curve χ_0 in the same figure). Hence products like $\eta_{12}{}^T\zeta_{13}$ which occur in (6.4) are rather unimportant: If r_{23} is small, then r_{12} and r_{13} are not very different, and the product $\eta^T(r_{12})\zeta(r_{13})$ is small because we cannot make r_{12} large while r_{13} remains of order c. If $r_{23}\gg c$, we may integrate over r_{13} essentially independently of r_{12}; then again the term $\zeta(r_{13})$ has little influence because it is appreciable only over such a small volume. Thus (6.4) reduces essentially to the simple expression

$$Z^{(1)T} \simeq \eta_{12}{}^T - \tfrac{1}{2}P_2(\hat{r}_{12}\cdot\hat{r}_{13})\eta_{13}{}^T. \qquad (6.5)$$

Dahlblom has confirmed this qualitative argument by calculating

$$F_T(r_{23}) = \int \eta^T(r_{12}) Z^{(1)T}(r_{12}, r_{23}, r_{13})\, d^3r_1 \qquad (6.6)$$

which is analogous to (5.20) and may be used to calculate W_T in (6.3). He finds that for all values of

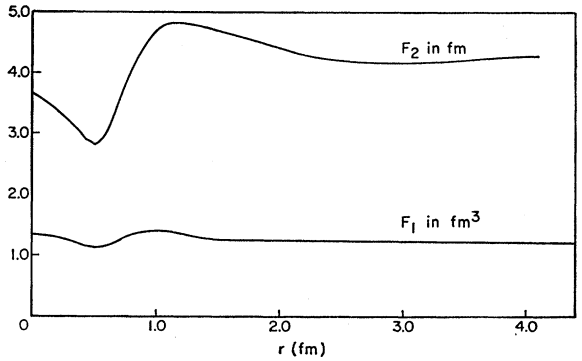

FIG. 17. The functions F_1 and F_2 defined in (5.20), (5.21). Both F_1 and F_2 are defined as $F=\frac{1}{2}[F(^1S)+F(^3S)]$, where $F(^1S)$ means that F is calculated using $\eta(^1S)$ and $\zeta(^1S)$.

[32] G. E. Brown and T. T. S. Kuo, Nucl. Phys. **85**, 40 (1966).

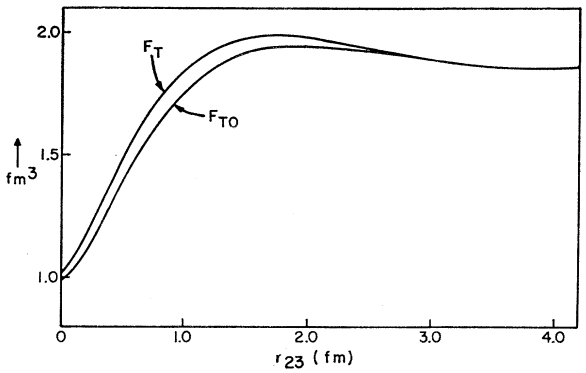

FIG. 18. The functions F_T and F_{T0} defined in the text, evaluated from Reid, hard-core potentials of 1965.

r_{23}, F_T is very close to

$$F_{T0}(r_{23}) = \int \eta^T(r_{12})[\eta^T(r_{12}) - \tfrac{1}{2}P_2(\hat{r}_{12}\cdot\hat{r}_{13})\eta^T(r_{13})]d^3r_1, \tag{6.7}$$

which corresponds to the approximation (6.5). Now this approximation does not contain ζ, and hence corresponds exactly to the third order of the Goldstone expansion. Thus, if the initial and final interaction are both *tensor*, the old-fashioned third order calculation of the three-body energy is adequate.

If (6.7) is inserted into (6.3), the first term $[\eta^T(r_{12})]^2$ corresponds to the "bubble" diagram 3(a), the second term to the "ring" diagram 3(b). For small r_{23} the ring diagram reduces the contribution from the bubble diagram by a factor of $\frac{1}{2}$ (this is exact for $r_{23}=0$ when $P_2=1$). For large r_{23} the ring contribution is essentially zero; explicit calculations show that it can be neglected beyond $r_{23}=2.5$ F (see Fig. 16). The middle interaction g_{23}, which has to be calculated for both even and odd states, therefore has a small weight for small r_{23} (where the repulsive part of the odd state forces is important) relative to larger r_{23} (where the attractive part of the even states is dominant). One can therefore expect that the three-body energy resulting from a tensor force in the initial and final interaction is attractive, and that the odd-state forces in the middle interaction do not contribute greatly.

The actual calculation was done employing Reid's hard core potential of 1965, the result being -1.7 MeV for g_{23} (total) and -2.2 MeV for g_{23} (even). This can be compared to $+1.1$ MeV if the initial and final interactions are central (see end of Sec. 5). The *total* three-body energy is then $-1.7+1.1=-0.6$, MeV which is very small indeed.

The resulting F_T and F_{T0}, defined by (6.6), (6.7) and calculated by Dahlblom, are given in Fig. 18.

Tensor Forces at Other Levels

We have only discussed the case when tensor forces act at the beginning and the end of the Goldstone diagram. At any intermediate level, we can have a tensor force act twice in succession on the same pair of particles: this gives an effective central force which can be treated like a central force (cf. item 3 near the end of Sec. 5).

Two tensor interactions between two *different* pairs of particles, at any two levels, give only a small contribution, because the average over spins give nearly zero. An exception is the case of an initial and final tensor interaction between different pairs, 12 and 13, which contributes the term $\eta(r_{13})$ in (6.5): as Dahlblom has shown, the relatively large effect of this is due to the fact that the momenta of the various particles are strongly correlated in this simple case which is not true in general.

Three tensor interactions, without any central ones, have been treated by Dahlblom *et al.*[33] using the OPEP interaction with a cut-off at 1 F. The result was only about $\frac{1}{2}$ MeV attraction.

7. SINGLE-PARTICLE POTENTIAL ENERGIES

We will now discuss the choice of the single-particle potential U (See A), which affects the value of the g matrix, and consequently every diagram in the expansion. In principle, of course, any convenient choice of U which gives a finite g matrix is permitted, but an educated choice that enhances the convergence of the Brueckner–Goldstone expansion is clearly preferable.

In simple physical terms, the potential U, which is added and subtracted from the total Hamiltonian, is supposed to reduce the size of the perturbation H_1 by absorbing some of the interparticle potential energy

$$\sum_{i\neq j} v_{ij}$$

into the unperturbed H_0. This would clearly enhance convergence. In diagrammatic language, the introduction of U results in some additional Goldstone diagrams besides the pure g matrix diagrams, and the choice of U is designed to cancel some of the latter by the former.

Thus, one choice of $U(b)$ for "particle" states[3] would be such as to cancel the third-order "particle–bubble" diagram [Fig. 19(b)] with the corresponding diagram

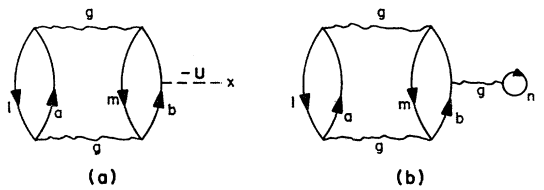

FIG. 19. The third-order "bubble diagram" and the third-order U diagram. Goldstone[3] suggested a choice of $U(b)$ designed to cancel these terms with one another.

[33] T. Dahlblom, K. G. Fogel, B. Quist, and A. Törn, Nucl. Phys. **56**, 177 (1964).

involving $U(b)$. In order to effect such a cancellation between Fig. 19(a) and 19(b) for a given value of momenta l, a, and m, we clearly require

$$U(b)=\sum_{n<k_F}\langle bn \mid g(W) \mid bn\rangle, \tag{7.1}$$

where W is the starting energy as defined in BBP[4] and in A. Now W and hence $\langle bn \mid g(W) \mid bn\rangle$ depend on the states l, m, and a, so that the choice $U(b)$ Eq. (7.1) is not a function of the state b alone. Thus, the cancellation of Fig. 19(a) by Fig. 19(b) for all l, m, and a, can be achieved only in an average sense, by choosing $U(b)$ as in Eq. (7.1) with some typical values of l, m, and a. This is precisely what BBP do in their choice of $U(b)$ for particle states. They not only try to cancel Fig. 19(b) on the average, but also the diagram with the middle g matrix exchanged. Thus, they choose

$$U(b)=\sum_{n<k_F}\{\langle bn \mid g(\Delta E) \mid bn\rangle-\langle bn \mid g(\Delta E) \mid nb\rangle\}, \tag{7.2}$$

with ΔE corresponding to $\langle l^2\rangle=\langle m^2\rangle=0.6k_F^2$ and $\langle a\rangle\sim 4\ \mathrm{F}^{-1}$ which are typical values. This choice is somewhat modified by including other third-order diagrams of comparable size as shown by Rajaraman.[14]

It should be noted that there is a self-consistency requirement implied in Eq. (7.2) since the $g(W)$ used to define $U(b)$ itself depends on $U(b)$. BBP define a self-consistent $U(b)$ according to the above prescription and show that this potential can be approximated by a quadratic form $A+Bb^2$, which agrees with the exact $U(b)$ in the important range of $b=2$ to $5\ \mathrm{F}^{-1}$. This is BBP's reference spectrum for particle states. Extensive work goes into the calculation of $U(b)$, ensuring self consistency, and the reader is referred to BBP and the subsequent work of Sprung[34] and Razavy[10,34] for details.

The BBP choice for the hole-state potential energy $U(m)$ is similar to (7.2), except for the important difference that the g matrices are on the energy shell.

$$U(m)=\sum_{n<k_F}\{\langle mn \mid g(W_0) \mid mn\rangle-\langle mn \mid g(W_0) \mid nm\rangle\}, \tag{7.3}$$

where $W_0=E_m+E_n$. This choice is simpler because it does not depend on the other particles in the diagram, unlike $U(b)$ in Eq. (7.1) where such a dependence arises because of the off-energy-shell nature. BBP also show, using an elegant identity generalized from an idea of Brueckner and Goldman,[35] that this choice of $U(m)$ cancels not only the "hole–bubble" diagram, but a whole sequence of diagrams shown in Fig. 20. There

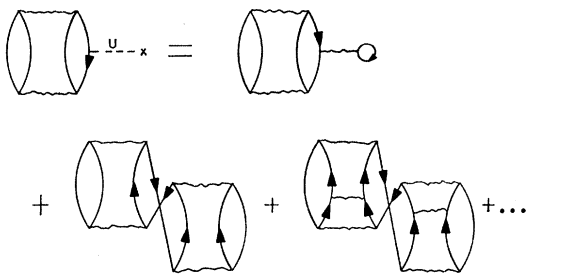

FIG. 20. Diagrams showing the absorption of a whole sequence of terms by the choice of the hole potential energies $U(m)$ on the energy shell.

is no corresponding identity for the particle energy $U(b)$ and the off-energy shell dependence of (7.2) has to be retained.

We will now show that, according to our present understanding of the subject, the choice of the particle potential energy $U(b)$ above should be modified. As mentioned in Sec. 3, at the time of the BBP work, it was hoped that the Brueckner–Goldstone expansion converges order by order. If this were so, then the first-order diagrams, using the BBP choice of $U(b)$ and $U(m)$, should give a good approximation to the binding energy since second-order diagrams do not exist and third-order diagrams are cancelled by the above potential energies. We now know from the subsequent research described in Secs. 3–6 that there is no convergence order by order in the g matrix, and that the third-order diagrams cancelled by $U(b)$ are the lowest-order terms in an alternating and nonconvergent series of three-body ladders. As Eqs. (4.23) and (4.26) show, the third-order terms are nearly three times the full three-body energy, and therefore, by cancelling them off, the BBP choice of $U(b)$ may do more harm than good.

On the other hand, the choice (7.3) of the hole energy $U(m)$ is still good because the diagrams in Fig. 20 that it absorbs do not belong to the three-body ladder sequence of Sec. 4. This can be readily seen by attempting to draw the diagrams in Fig. 18 in the ladder notation. Thus, we will retain the BBP choice of $U(m)$ which absorbs Goldstone diagrams not summed in the three-body energy, but look for alternate prescriptions for the particle potential $U(b)$.

Several choices have been suggested in the literature. We have mentioned, in Sec. 3, that the Coon and Dabrowsky choice[17] amounts to the BBP prescription. More recently Brandow[1] has suggested that $U(b)=0$ be used. This is appealing not only because of its simplicity but because it gives a sizeable energy gap between particle and hole spectra, thus facilitating the use of the reference method. [The average value of $U(m)$ is around -90 MeV.] Moreover, the small result obtained by Dahlblom for the complete 3-body energy, -0.6 MeV (cf. end of Sec. 6), makes the use of $U(b)=0$ probably a very good approximation.

[34] M. Razavy and D. W. L. Sprung, Phys. Rev. **133**, B300 (1964).

[35] K. A. Brueckner and D. T. Goldman, Phys. Rev. **117**, 207 (1960).

On the other hand, the Brandow choice does not absorb any specific higher-order correction terms. Thus the problem of evaluating four-body corrections etc. is still left open.

Bethe[6] has suggested that $U(b)$ be defined so as to absorb the full three-body energy evaluated in Sec. 4. In other words, $U(b)$ should be chosen such that the three-body energy may be written as

$$W_3=\int |\, y(\mathbf{b})\,|^2 U(\mathbf{b})\, d^3b, \tag{7.4}$$

where

$$y(\mathbf{b})=\int \eta(\mathbf{r})\, \exp\,(i\mathbf{b}\cdot\mathbf{r})\, d^3r \tag{7.5}$$

and $|\, y(\mathbf{b})\,|^2$ is the probability that a pair of nucleons is excited from a state in the Fermi sea to a state of momenta $+\mathbf{b}$ and $-\mathbf{b}$ (the momenta of the initial hole states have been neglected, and η has been assumed independent of these momenta). Obviously (7.4) is only one condition on the function $U(b)$ which still permits wide latitude in its choice. Bethe[6] proposed to set

$$U(b)=|\, y(b)\,|^{-2}\int d^3r_{23} g(b, r_{23}) F_1(r_{23}), \tag{7.6}$$

with F_1 given by (5.20). At least approximately, this should satisfy (7.4). Using this prescription, Kirson[12] and Sprung, Bhargava, and Dahlbolm[27] have calculated $U(b)$, and the latter workers also include to some extent the effect of tensor forces.

Equation (7.6) may be criticized on five counts: (1) It is not established by any fundamental theory. (2) It is not even proved to satisfy (7.4). (3) It has a singularity if $y(b)=0$ for some b. (4) Sprung *et al.*[27] found that for b slightly greater than k_F, $U(b)$ tended to become smaller than $U(m)$ for states m slightly below k_F, thus giving a "negative gap" in the energy spectrum. They arbitrarily removed this unacceptable negative gap. (5) In three-body ladder diagrams, all three nucleons are interacting with each other, and it is therefore somewhat artificial to treat this effect as a single-particle potential on one of them.

A more systematic definition of $U(b)$ has recently been given by Bethe.[29] He starts from our Eq. (5.13) and finds

$$U(b)=[y(b)]^{-1}\int d^3r_{23} g_{Pk}{}^*(r_{23})\, Y_b(r_{23}), \tag{7.7}$$

$$Y_b(r_{23})=\int d^3r_{12}\, j_0(br_{12}) Z^{(1)}(r_{12}, r_{23}, r_{31}). \tag{7.8}$$

For the values of b which are most important according to Kirson, viz. $b\approx 0.6/c$, $r_{12}\, j_0(br_{12})$ has its peak at about the same value of r_{12} as $\eta(r_{12})$; then $Y_b(r_{23})$ is proportional to F_1, Eq. (5.20), and the new definition (7.7) of $U(b)$ reduces to the old one, (7.6). On the other hand, for small b, j_0 in (7.8) is ≈ 1 so that Y_b is nearly independent of r_{23} (while for larger b, Y_b increases with r_{23}); therefore, for small b, the repulsive contribution from $r_{23}\leq c$ in (7.7) is not suppressed by the factor Y_b. This automatically eliminates the negative energy gap of Sprung *et al.*, discussed as point 4 above. Points 1 and 2 are clearly satisfied by the new definition (7.7); point 5 of course remains.

The problem about the denominator $y(b)$ is removed by remembering that the initial interaction may be alternatively tensor or central. Then it can easily be shown that a suitable definition is

$$U(b)=\frac{y_c^2(b)\, U_c(b)+y_T^2(b)\, U_T(b)}{y_c^2(b)+y_T^2(b)}, \tag{7.9}$$

where $y_c(b)$ and $y_T(b)$ are the expressions (7.5), calculated, respectively, with the defect functions η_c and η_T for central and tensor forces, and U_c, U_T are defined correspondingly. The denominator of (7.9) does not vanish for any b, so that criticism 3 above is now also taken care of.

Multi-Particle Clusters

Rajaraman[13] has emphasized the usefulness of defining a $U(b)$ in order to absorb the principal effect of many-body clusters. His argument runs briefly as follows: Consider all three-body ladders to be divided into the three groups as suggested in Sec. 3: (i) those involving g_{short} only, (ii) those with v_l only, and (iii) those mixed in g_s and v_l. For class (i), we expect the four-body energy to be much smaller than the three-body energy and so on, because of the short-rangedness of the force ($pc^3<1$). The class (ii) diagrams are similar to higher Born terms in v_l and should be very small since even the second Born term $v_l(Qv/e)_l$ is only 2% of the first Born term.[11,12] This then leaves diagrams of class (iii) as the leading contributors to the four-body energy and larger clusters. In fact, even for the three-body energy of about -5 MeV, we will show that the dominant contribution comes from a diagram of this class.

Now, for any typical potential, such as the standard hard-core potential, the matrix element $\langle \mathbf{k}\,|\, v_l\,|\,\mathbf{k}_0\rangle$ is strongly dependent on the momentum transfer $\mathbf{q}=\mathbf{k}-\mathbf{k}_0$, although the diagonal element $\langle \mathbf{k}\,|\, v_l\,|\,\mathbf{k}\rangle$ is relatively independent of k. A graph of $\langle \mathbf{k}\,|\, v_l\,|\,\mathbf{k}_0\rangle$ for $k_0=(0.3)^{1/2}k_F$ is given in Fig. 21, and shows that a typical off-diagonal matrix element is about $\frac{1}{7}$, or less, of the diagonal one. This, for instance, is the reason why the second-order term in v_l, namely, $v_l(Qv/e)_l$, is only 2% of the first-order v_l. The former contains two off-diagonal matrix elements compared to the diagonal first-order term. On the other hand, the dependence of g_s on the momentum transfer is not strong.

From this, we would expect that the most important diagrams of class (iii) should involve diagonal elements of v_l. A diagonal matrix element in a Goldstone diagram corresponds to "bubble interactions." Thus, we would expect a diagram of the type in Fig. 22(a) to be larger than the one in 22(b), although both belong to class (iii) and are four-body terms. In addition, a diagram with a bubble interaction contains one less excited particle, and hence smaller energy denominators, which also enhances its importance. It should be noted here that if one uses a Serber force for v_l instead of a Wigner

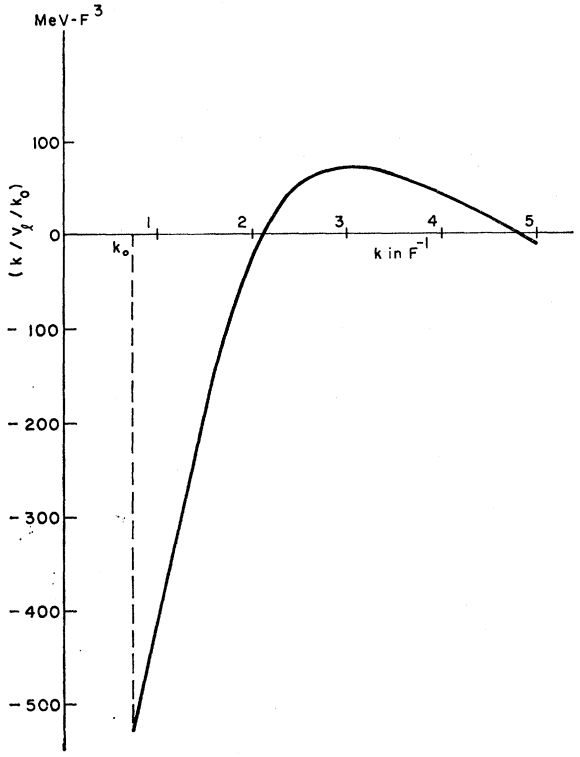

FIG. 21. Dependence of the long-range force matrix elements on the momentum transfer.

force, then the exchange of the bubble interaction is also important. The best way to take into account diagrams of the type in Fig. 22(a) with exchanges is to absorb them into the single-particle energy with a potential

$$U_{\text{long}}(b)=\sum_{n<k_F}\langle bn \mid v_l \mid bn\rangle-\tfrac{1}{4}\langle bn \mid v_l \mid nb\rangle. \quad (7.10)$$

The factor of $-\frac{1}{4}$ in front of the exchange term arises for spin-independent forces because of the statistical weight arguments given earlier.[14] For Serber forces, of course,

$$\langle bn \mid v_l \mid nb\rangle=\langle bn \mid v_l \mid bn\rangle \quad (7.10a)$$

if states b and n agree in spin and isospin.

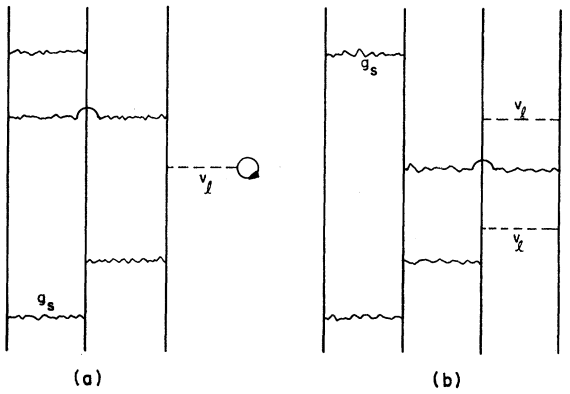

FIG. 22. Two four-body terms. Diagram (a) contains one diagonal v matrix element while (b) has two off-diagonal ones.

Rajaraman[13] also showed that the third-order, long-range bubble diagram of Fig. 23 gives about as much energy (−5 MeV) as the total three-body interaction as calculated by Kirson,[12] at least if the "standard hard core potential" is used. Accordingly, Rajaraman[13] proposed to use only the long-range bubble terms in the definition of $U(b)$. However, if this were taken literally, this would enhance the trouble found by Sprung *et al.* and listed as criticism, point 4 above. The new Bethe prescription (7.7) or (7.9) also emphasizes the long-range force, and is therefore acceptable from the point of view of Rajaraman.

Since Rajaraman has shown that bubble interactions involving v_l give the main contribution to the many-body energy, we may expect that the use of (7.9) for $U(b)$ will absorb a major part of these many-body clusters. The prescription for nuclear matter calculations is then the same as has been used in the past by Brueckner's group and others, viz:

Calculate the two-body g matrix from the integral equation

$$g \mid mn\rangle=v \mid mn\rangle-(2\pi)^{-3}\int d^3bv \mid ab\rangle \times\frac{Q(a,b)}{T(a)+T(b)+U(a)+U(b)-E(m)-E(n)} \times\langle ab \mid g \mid mn\rangle, \quad (7.11)$$

where $T(a)$ is the kinetic and $U(a)$ the potential energy of the particle state a, and $E(m)$ the total energy of a hole state m. Similar prescriptions hold if the initial

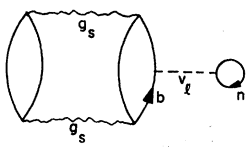

FIG. 23. The long-range "bubble" diagram which dominates the three-body energy.

state includes one or two particles rather than two holes. Calculate $U(b)$ from (7.9).

Summing the diagonal elements of g, we get the total, two-body nuclear energy. If now the denominator of (7.11) is expanded in powers of $U(a)+U(b)$, the term independent of U will give the two-body energy according to Brandow's prescription.[1] The term linear in $U(a)+U(b)$ will give the three-body energy because U satisfies (7.4). The remainder represents the part of the multi-body energy which we can take into account by our simple scheme. This remainder then is the only term by which our prescription differs from Brandow's if both are consistently carried out. Simple algebra shows that our prescription will provide more attraction than his. This will be especially important for the low particle states, with b slightly above k_F, which are reached mostly by the tensor force. We guess that the effect of putting $U(a)+U(b)$ into the denominator of (7.11) may be about 1 MeV. This attraction is, however, already contained in calculations such as that of Sprung *et al.*,[27] so that it cannot be invoked to give a larger binding energy than previously found.

ACKNOWLEDGMENT

One of us (R.R.) is indebted to Dr. Ben Day for useful conversations and for his cooperation in tailoring this work along with his preceding article so as to supplement one another.

APPENDIX. ERRORS IN PREVIOUS DEFINITIONS

Bethe[6] originally proposed to use in (7.6) not the factor $F_1(r_{23})$ but the ratio[36]

$$f_b(r_{23})=F_1(r_{23})/F_a(r_{23}), \tag{A1}$$

where F_a is the expression for F_1 in third order, which is given by (4.28), viz.,

$$F_a(r_{23})=\int d\tau_1\eta(r_{12})[\eta(r_{12})+\eta(r_{13})]. \tag{A2}$$

His argument was that $g(b, r_{23})$ in (7.6) was calculated originally by considering the third-order diagrams only, that the third-order diagrams contain the factor (A2) as explained near (4.24), and that therefore the g should be multiplied by the factor (A1).

This argument is wrong.[37] To see this, we consider the third-order diagrams. A complete list of these was given by Rajaraman.[14] Excluding the interaction with the potential U [our Fig. 19(b)] and the hole–hole interaction [Fig. 3(d)], there are 12 diagrams which involve three-body interactions. Of these, ten involve exchanges of some kind between the three particles, and therefore contribute only if at least two particles agree in spin and isospin; hence these diagrams have smaller statistical weight (by factors of $\frac{1}{4}$ or 16) than the remaining two diagrams. These two are the bubble and the ring diagrams, Fig. 3(a) and 3(b) of our paper, and we shall consider only these.

The bubble diagram may be written as

$$B=\int \eta(r_{12})g(r_{23})\eta(r_{12})d\tau_2d\tau_3 \tag{A3}$$

and the ring diagram as

$$R=\int \eta(r_{12})g(r_{23})\eta(r_{13})d\tau_2d\tau_3. \tag{A4}$$

In each case, the interactions have been enumerated in the order of their occurrence in the diagram. If $P_{ik}{}^M$ denotes the Majorana exchange operator for particles i and k, (A4) may be written as

$$R=\int \eta(r_{12})g(r_{23})P_{23}{}^M\eta(r_{12})d\tau_2d\tau_3. \tag{A5}$$

Here g and P^M should be considered as operators operating on the "wave function" following them; g, for instance, may be different for each angular momentum state. Adding (A3) and (A5) gives

$$R+B=\int \eta(r_{12})g(r_{23})(1+P_{23}{}^M)\eta(r_{12})d\tau_2d\tau_3. \tag{A6}$$

The operator $1+P_{23}{}^M$ selects from η only the part which is even in r_{23}; therefore only the part of g which operates on even angular momenta will contribute. We may rewrite (A6)

$$R+B=\int \eta(r_{12})g_{\text{even}}(r_{23})(1+P_{23}{}^M)\eta(r_{12})d\tau_2d\tau_3. \tag{A7}$$

The operator $1+P^M$ should, however, not be left out (replaced by 2, as would seem natural in combination with states even in r_{23}) because it operates on a function which also depends on r_1, and

$$(1+P_{23}{}^M)\eta(r_{12})=\eta(r_{12})+\eta(r_{13})\neq 2\eta_{12}. \tag{A8}$$

Exchange terms reduce (A7) exactly to one-half, as was shown by Rajaraman[14] and Bethe[6]:

$$R+B+\text{exchange}=\tfrac{1}{2}(R+B). \tag{A9}$$

We may now treat $R+B$ in several different ways. One is to integrate first over r_1; then

$$R+B=\int g_{\text{even}}(r_{23})d\tau_{23}F_a(r_{23}), \tag{A10}$$

with F_a defined by (A2). Another method is to expand

[36] Our quantities F_1, F_a were denoted by F and F_1, respectively, in Ref. 6. We apologize.

[37] One of us (H.A.B.) is grateful to Dr. Dahlblom for discussions which led directly to the discovery of this error.

the η's in Fourier integrals; thus

$$\eta(r_{12}) = (2\pi)^{-3} \int d^3b \exp\left[i\mathbf{b}(\mathbf{r}_1-\mathbf{r}_2)\right] y(b),$$

$$\eta(r_{12})\eta(r_{13}) = (2\pi)^{-6} \int d^3b d^3b' y^*(b) y(b')$$

$$\times \exp\left[-i\mathbf{b}\cdot(\mathbf{r}_1-\mathbf{r}_2)\right] \exp\left[i\mathbf{b}'\cdot(\mathbf{r}_1-\mathbf{r}_3)\right].$$

Integration over $d\tau_1$ gives $(2\pi)^3\delta(\mathbf{b}-\mathbf{b}')$ so that

$$\int \eta(r_{12})\eta(r_{13})\, d\tau_1 = (2\pi)^{-3} \int d^3b \mid y(b) \mid_2 \exp(i\mathbf{b}\cdot\mathbf{r}_{23}) \tag{A11}$$

and

$$R+B = (2\pi)^{-3} \int d^3b \mid y(b) \mid^2 G(b), \tag{A12}$$

$$G(b) = \int d\tau_{23} g_{\text{even}}(r_{23}) \left[1+\exp(i\mathbf{b}\cdot\mathbf{r}_{23})\right],$$

$$= \int d\tau_{23} g_{\text{even}}(r_{23}) (1+\cos \mathbf{b}\cdot\mathbf{r}_{23}). \tag{A13}$$

In the form (A12), $R+B$ may be considered as the effect of a bubble diagram, Fig. 3(a), alone, with $y(b)$ representing the first and the last interaction including the adjacent propagators, and $G(b)$ the middle interaction. In $G(b)$, the term $\cos \mathbf{b}\cdot\mathbf{r}_{23}$ comes, of course, originally from the ring diagram 3(b), and represents an interaction in which particles 2 and 3 exchange their momenta.[38] The fact that (A12) has the form of a bubble diagram alone, is of course most useful because it permits us to consider $G(b)$ as an insert in a particle line. The sum of $G(b)$ over all states n in the Fermi sea is then the effective potential $U(b)$, and this in turn may be used in the first-order calculation of the interaction between the "hole states" l and m. This treatment of all the third-order diagrams as inserts was indeed the aim of Rajaraman's paper.[14]

The effective interaction, $G(b)$ of (A13), will depend on b even if the fundamental interaction, $g_{\text{even}}(r_{23})$, does not explicitly depend on momentum.[39] The exchange term, $\cos \mathbf{b}\cdot\mathbf{r}_{23}$, decreases with increasing b, especially for larger r_{23}: this means that the attractive force gets weaker while the repulsive core remains nearly at full strength for high b.

In this way, the form (A12) reflects the properties of the alternative form (A10) of the third-order interaction. As Figs. 14 and 15 show, F_a has a substantial maximum at small r, emphasizing the effect of the repulsive core. In $G(b)$ likewise, at least for the larger b, the short-range interaction has greater weight than the long-range part.

The mistake made in Ref. 6 was based on the belief that

$$G(b) = \int g_{\text{even}}(r)\, d\tau. \tag{A14}$$

As we have shown, both in (A10) and (A13), this belief was wrong. It was then argued[6] that the full three-body interaction differs from the third order by the factor f_b, Eq. (A1). This is correct, but when applied to the correct expression (A10), it gives the correct result (correct if g does not explicitly depend on b)

$$W_3 = \int g_{\text{even}}(r) F_1(r)\, d\tau. \tag{A15}$$

In Ref. 6, starting from the wrong third-order expression (A14), the incorrect statement was made that

$$W_3(\text{Ref. 6}) = \int g_{\text{even}}(r) f_b(r)\, d\tau. \tag{A16}$$

One of the authors (H.A.B.) must apologize for this bad error which he made in Ref. 6, and which has crept into all the following work, such as Kirson's thesis[12] and Sprung and Bhargava.[8,24] The numerical consequences of the present correction are very serious.

Dahlblom[40] has calculated the three-body interaction using the correct formulas, (5.20) to (5.22), using Reid's hard-core potential of 1965. Taking into account only an initial (and final) *central* interaction, he finds a three-body energy of +1.1 MeV. The inclusion of initial tensor interaction reduces this result to −0.6 MeV (see end of Sec. 6). For comparison, Sprung,[41] using the same potential, finds about −5 MeV for

[38] To see this in more detail, we use an argument similar to Ref. 14. The middle interactions in Figs. 3(a) and 3(b) both start with particle 2 in state b, and 3 in state n. In Fig. 3(a), their states remain unchanged after the interaction. But in 3(b), particle 2 goes into state m and 3 into state c. Assuming now that the momenta m, n of the hole states are small compared with those of the particle states b, c, we have $m \approx n$ and, because of momentum conservation, $c \approx b$. Hence, in the middle interaction of Fig. 3(b), the two particles essentially exchange their momenta, the momentum changes being approximately $+\mathbf{b}$ and $-\mathbf{b}$.

[39] This result and Eq. (A13) are not new, but (A13) is exactly the same expression as is used in BBP for a Serber force interaction. In BBP (7.18) this is shown to be (apart from numerical factors)

$$G = \int v(r)\left[1+j_0(2k_0 r)\right] d\tau. \tag{a}$$

If in (A13) we replace $g(r)$ by $v(r)$, integrate over angles, and remember that $b = 2k_0$, we get exactly (a). So (A12), (A13) are in exact accord with previous calculations of the third-order interactions. What is new is merely that an alternative way of writing the third-order contribution is (A10).

[40] T. Dahlblom (private communication).

[41] D. W. L. Sprung (private communication).

initial central interaction alone. Thus the correct treatment of three-body forces appears to reduce this part of the binding energy by 6 MeV, destroying the approximate agreement with observation which had been achieved by Sprung and Bhargava.[8]

The reason for this "loss of attraction" is easy to see. As we already pointed out, the "third-order" correlation function F_a has a strong maximum for small r (see Figs. 14, 15). Hence the ratio f_b, Eq. (A1), is small at short distances r. Hence, in the old, erroneous theory (A16), the contribution of the core is strongly suppressed. On the other hand, F_1 itself, in Fig. 15, is nearly constant for all r; there is no appreciable core suppression; hence the correct result (A15) is more repulsive.

This effect is very pronounced for the Reid hard-core potential (Fig. 15) which was used by Dahlblom and Sprung. The standard hard-core potential, used by Kirson, gives the results of Fig. 14: Here F_a is only 1.3 at $r=0$ so that the difference between using (A15) and (A16) should be less great. Hence Kirson's estimate $W_3=-5$ MeV is probably not *too* bad for his potential.

It should be noted that there is, of course, still much less repulsion in the correct W_3, (A15), than in the pure third-order calculation. Equation (A10) gives its result; here the core contribution is enhanced because F_a has a maximum for small r. Thus the correct theory of three-body interactions still has a beneficial effect: It removes the core enhancement which the third-order theory would give.

It should also be remembered that, for a soft-core potential, the three-body interaction should not be so important.[6] Thus the loss of binding, compared with Sprung and Bhargava, will probably be considerably less. There is then still hope for agreement of the calculated binding energy with observation for a soft core.[42]

There is one practical advantage in these, otherwise disturbing, new results: The three-body energy seems to be close to zero. It is then a good approximation to set the potential energy of all intermediate ("particle") states to zero. The advantage of this procedure has been pointed out particularly by Brown and his collaborators.[43]

---

[42] C. W. Wong, in his thesis (Harvard University), first emphasized the importance of the soft core. This importance seems to have further increased.

[43] G. E. Brown and T. T. S. Kuo, Nucl. Phys. **85**, 40 (1966).